CHAPTER 7

Principles of Stability and Control

An important problem to aviation is . . . improvement in the form of the aeroplane leading toward natural inherent stability to such a degree as to relieve largely the attention of the pilot while still retaining sufficient flexibility and control to maintain any desired path, without seriously impairing the efficiency of the design.

From the First Annual Report
of the NACA, 1915

7.1 INTRODUCTION

The scene: A French army drill field at Issy-les-Moulineaux just outside Paris. *The time:* The morning of January 13, 1908. *The character:* Henri Farman, a bearded, English-born but French-speaking aviator, who had flown for his first time just four months earlier. *The action:* A delicately constructed Voisin-Farman I-bis biplane (see Fig. 7.1) is poised, ready for the takeoff in the brisk Parisian wind, with Farman seated squarely in front of the 50-hp Antoinette engine. The winds ripple the fabric on the Voisin's box kite–shaped tail as Farman powers to a bumpy liftoff. Fighting against a head wind, he manipulates his aircraft to a marker 1000 m from his takeoff point. In a struggling circular turn, Farman deflects the rudder and mushes the biplane around the marker, the wings remaining essentially level to the ground. Continuing in its rather wide and tenuous circular arc, the airplane heads back. Finally, Farman lands at his original takeoff point,

PREVIEW BOX

Imagine that you have designed your own airplane and you are ready to fly it for the first time. You have followed the principles laid out in the previous chapters of this book, and you are confident that your airplane will fly as fast, as high, as far, and as long as you have planned. With confidence, you take off and begin the first flight of your new design. Within moments after takeoff, you hit a gust of wind that momentarily pitches the airplane up, literally rotating the airplane to a higher-than-intended angle of attack. Now what? Are you going to have to fight to bring your airplane under control, or will it automatically return to its previous orientation after a few moments? Indeed, have you properly designed your airplane so that it will return to its original orientation? How do you do that? That is, how do you insure that your airplane, when disturbed by the gust of wind, will not continue to pitch up and completely go out of control? These are truly important questions, and you will find answers in this chapter. The questions and answers have to do with airplane *stability,* a major subject of this chapter.

Assume that your airplane is stable; that is, it will automatically return to its original orientation after experiencing some type of disturbance. As you are flying, you wish to speed up, but also maintain level flight. You know from our conversations in Chap. 6 that you must correspondingly reduce the angle of attack. This can be accomplished by changing the elevator deflection on the tail. But how much do you need to deflect the elevator? And how much force must you exert on the elevator to get it to deflect the proper amount? These questions may seem somewhat mundane, but if you do not know the proper answers and you did not properly account for them in your design, most likely you will not be able to control your airplane. The second major subject of this chapter is airplane *control,* where you will find answers to these questions.

If airplanes are unstable and/or if they are uncontrollable, they will most likely crash. This is serious business. This is a serious chapter. Please read it with some care. At the same time, however, I predict that you will enjoy reading this chapter because it takes you into new territory associated with the flight of airplanes, with some different physics and different mathematics than we have previously considered.

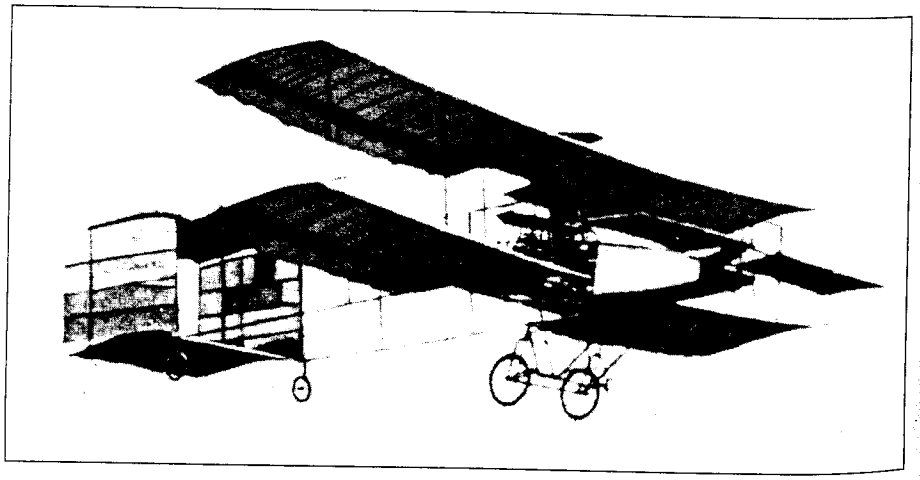

Figure 7.1 The Voisin-Farman I-bis plane.
(Source: *National Air and Space Museum.*)

amid cheers from the crowd that had gathered for the occasion. Farman has been in the air for 1 min 28 s—the longest flight in Europe to that date—and has just performed the first circular flight of 1-km extent. For this, he is awarded the Grand Prix d'Aviation. (Coincidentally, in the crowd is a young Hungarian engineer, Theodore von Karman, who is present only due to the insistence of his female companion—waking at 5 AM in order to see history made. However, von Karman is mesmerized by the flight, and his interest in aeronautical science is catalyzed. Von Karman will go on to become a leading aerodynamic genius of the first half century of powered flight.)

The scene shifts to a small racetrack near Le Mans, France. *The time:* Just seven months later, August 8, 1908. *The character:* Wilbur Wright, intense, reserved, and fully confident. *The action:* A new Wright type A biplane (see Fig. 1.25), shipped to France in crates and assembled in a friend's factory near Le Mans, is ready for flight. A crowd is present, enticed to the field by much advance publicity and an intense curiosity to see if the "rumors" about the Wright brothers' reported success were really true. Wilbur takes off. Using the Wrights' patented concept of twisting the wing tips (*wing warping*), Wilbur is able to bank and turn at will. He makes two graceful circles and then effortlessly lands after 1 min 45 s of flight. The crowds cheer. The French press is almost speechless but then heralds the flight as epoch-making. European aviators who witness this demonstration gaze in amazement and then quickly admit that the Wrights' airplane is far advanced over the best European machines of that day. Wilbur goes on to make 104 flights in France before the end of the year and in the process transforms the direction of aviation in Europe.

The distinction between these two scenes, and the reason for Wilbur's mastery of the air in comparison to Farman's struggling circular flight, involves stability and control. The Voisin aircraft of Farman, which represented the best European state of the art, had only rudder control and could make only a laborious, flat turn by simply swinging the tail around. In contrast, the Wright airplane's wing-twisting mechanism provided control of roll, which when combined with rudder control, allowed effortless turning and banking flight, figure-eights, etc. Indeed, the Wright brothers were *airmen* (see Chap. 1) who concentrated on designing total control into their aircraft before adding an engine for powered flight. Since those early days, airplane stability and control have been dominant aspects of airplane design. This is the subject of this chapter.

Airplane performance, as discussed in Chap. 6, is governed by forces (along, and perpendicular to, the flight path), with the translational motion of the airplane as a response to these forces. In contrast, airplane stability and control, discussed in this chapter, are governed by moments about the center of gravity, with the rotational motion of the airplane as a response to these moments. Therefore, moments and rotational motion are the main focus of this chapter.

Consider an airplane in flight, as sketched in Fig. 7.2. The center of gravity (the point through which the weight of the complete airplane effectively acts) is denoted as cg. The xyz orthogonal axis system is fixed relative to the airplane; the x axis is along the fuselage, the y axis is along the wingspan perpendicular to

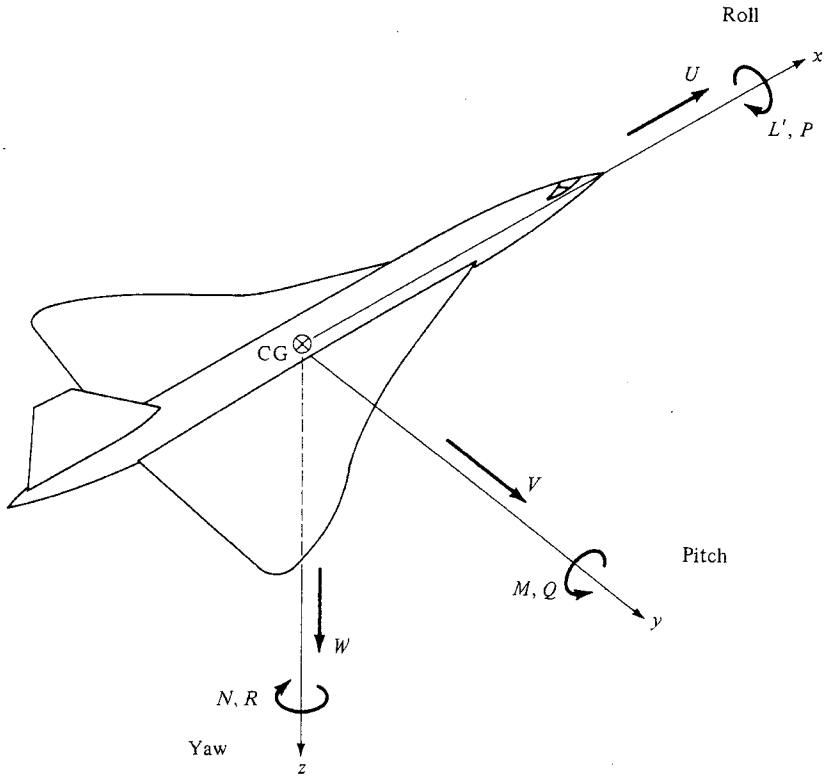

Figure 7.2 Definition of the airplane's axes along with the translational and rotational motion along and about these axes.

the x axis, and the z axis is directed downward, perpendicular to the xy plane. The origin is at the center of gravity. The translational motion of the airplane is given by the velocity components U, V, and W along the x, y, and z directions, respectively. (Note that the resultant free-stream velocity V_∞ is the vector sum of U, V, and W.) The rotational motion is given by the angular velocity components P, Q, and R about the x, y, z axes, respectively. These rotational velocities are due to the moments L', M, and N about the x, y, and z axes, respectively. (The prime is put over the symbol L so that the reader will not confuse it with lift.) Rotational motion about the x axis is called *roll;* L' and P are the *rolling* moment and velocity, respectively. Rotational motion about the y axis is called *pitch;* M and Q are the *pitching* moment and velocity, respectively. Rotational motion about the z axis is called *yaw;* N and R are the *yawing* moment and velocity, respectively.

There are three basic controls on an airplane—the ailerons, elevator, and rudder—which are designed to change and control the moments about the x, y, and z axes. These control surfaces are shown in Fig. 2.14 and repeated in Fig. 7.3; they are flaplike surfaces that can be deflected back and forth at the

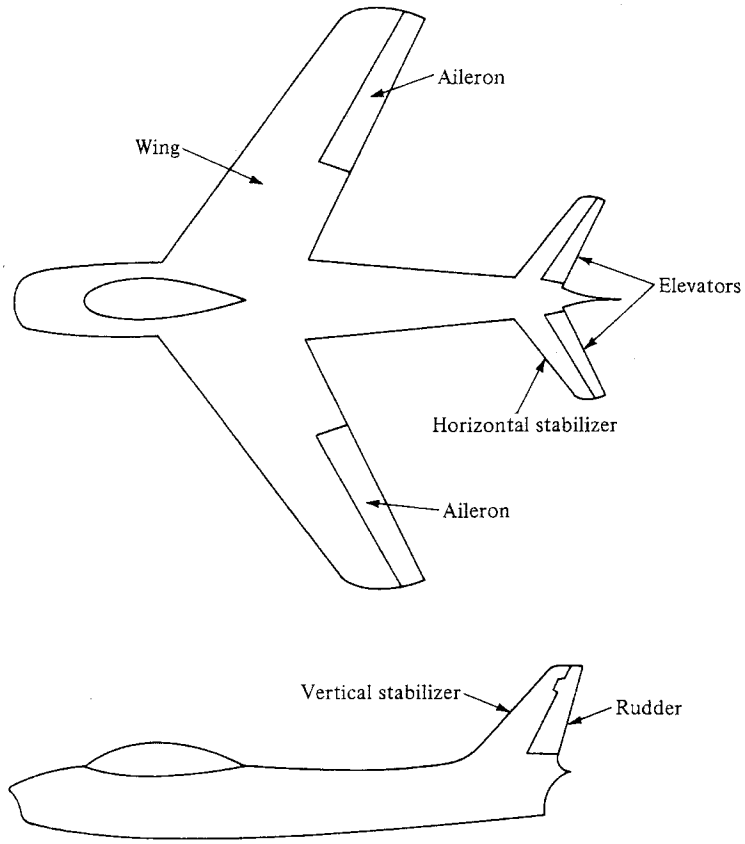

Figure 7.3 Some airplane nomenclature.

command of the pilot. The ailerons are mounted at the trailing edge of the wing, near the wing tips. The elevators are located on the horizontal stabilizer. In some modern aircraft, the complete horizontal stabilizer is rotated instead of just the elevator (so-called flying tails). The rudder is located on the vertical stabilizer, at the trailing edge. Just as in the case of wing flaps discussed in Sec. 5.17, a downward deflection of the control surface will increase the lift of the wing or tail. In turn, the moments will be changed, as sketched in Fig. 7.4. Consider Fig. 7.4*a*. One aileron is deflected up and the other down, creating a differential lifting force on the wings, thus contributing to the rolling moment L'. In Fig. 7.4*b*, the elevator is deflected upward, creating a negative lift at the tail, thus contributing to the pitching moment M. In Fig. 7.4*c*, the rudder is deflected to the right, creating a leftward aerodynamic force on the tail, thus contributing to the yawing moment N.

Rolling (about the x axis) is also called *lateral motion*. Referring to Fig. 7.4*a*, we see that ailerons control roll; hence, they are known as *lateral controls*.

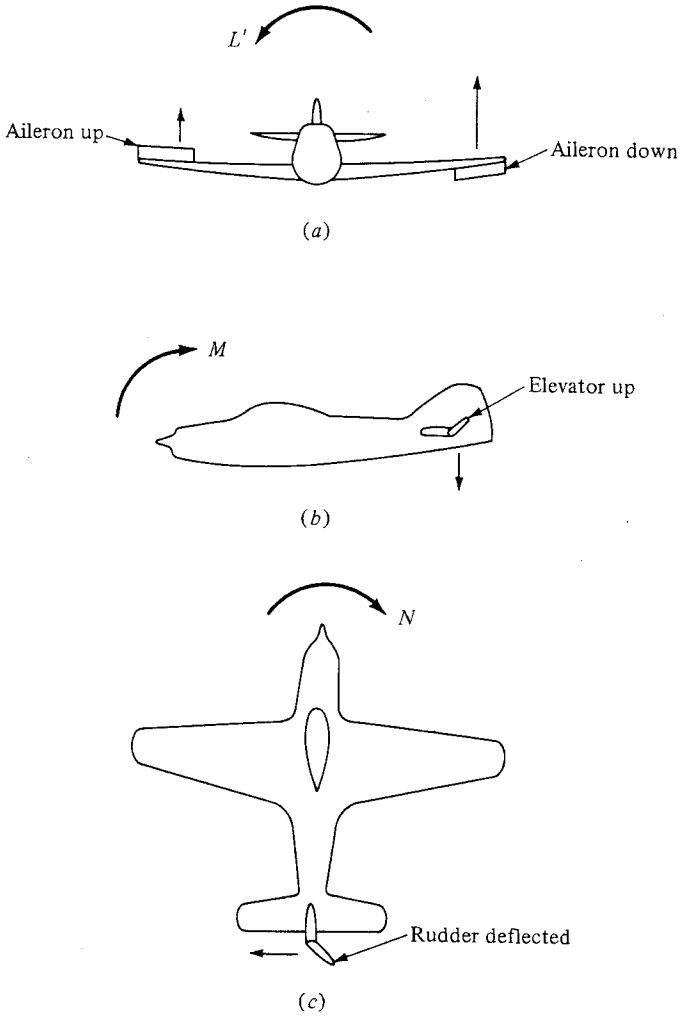

Figure 7.4 Effect of control deflections on roll, pitch, and yaw. (*a*) Effect of aileron deflection; lateral control. (*b*) Effect of elevator deflection; longitudinal control. (*c*) Effect of rudder deflection; directional control.

Pitching (about the y axis) is also called *longitudinal motion.* In Fig. 7.4*b*, we see that elevators control pitch; hence, they are known as *longitudinal controls.* Yawing (about the z axis) is also called *directional motion.* Figure 7.4*c* shows that the rudder controls yaw; hence, it is known as the *directional control.*

All these definitions and concepts are part of the basic language of airplane stability and control; they should be studied carefully. Also, in the process, the following question emerges: What is meant by the words *stability and control* themselves? This question is answered in Sec. 7.2.

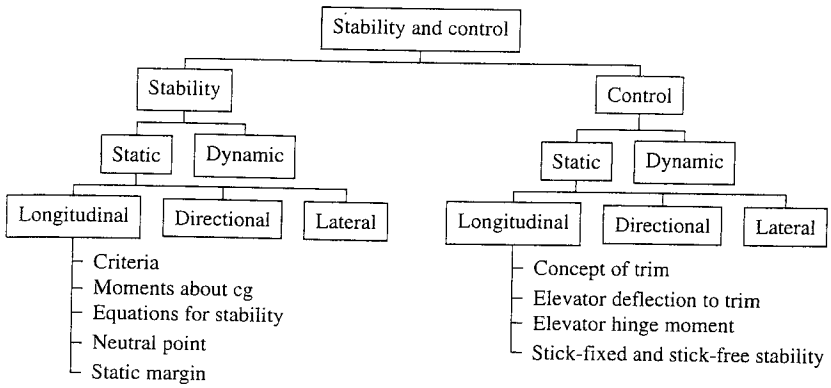

Figure 7.5 Road map for Chap. 7.

Return to the general road map for this book, shown in Fig. 2.1. With this chapter, we are still dealing with the overall subject of flight mechanics, but now we are concentrating on the second subbox under flight mechanics, namely, stability and control. The road map for the present chapter is shown in Fig. 7.5. There are two general routes shown, that for stability in the left column and that for control in the right column. Both the subjects of stability and control can be subdivided into categories labeled *static* and *dynamic*, as shown in Fig. 7.5. We define the difference between these categories in the next section. In this chapter we concentrate primarily (though not exclusively) on longitudinal stability and control. We deal with such considerations of static longitudinal stability as the calculation of longitudinal moments about the center of gravity, equations that can be used to help us determine whether an airplane is stable or not; and we define two concepts used to describe the stability characteristics, namely, the neutral point and the static margin. For the latter part of this chapter, we run down the right side of the road map in Fig. 7.5, dealing primarily with static longitudinal control. Here we examine the concept of *trim* in greater detail, and we look at elevator deflections necessary to trim and the associated hinge moments for the elevator. We also look at the differences between *stick-fixed* and *stick-free* stability. Many of the terms used may seem unfamiliar and somewhat strange. However, we spend the rest of this chapter helping you to learn these concepts and making you more familiar with the language of airplane stability and control. It will be useful for you to frequently return to Fig. 7.5 as we proceed through this chapter, to help orient yourself about the details and where they fit into the bigger picture.

7.2 DEFINITION OF STABILITY AND CONTROL

There are two types of stability: static and dynamic. They can be visualized as follows.

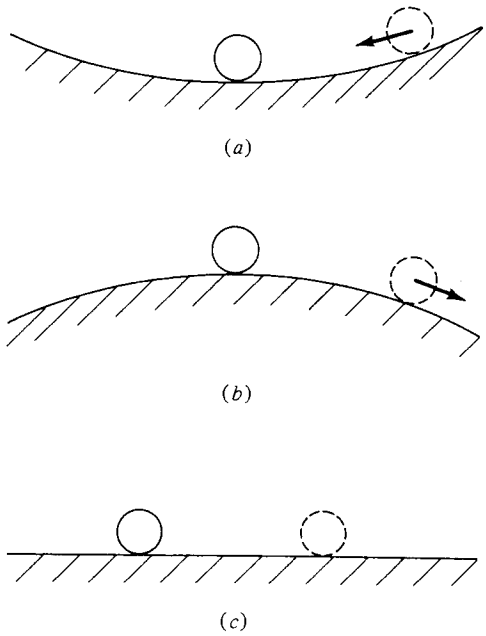

Figure 7.6 Illustration of static stability. (*a*) Statically stable system. (*b*) Statically unstable system. (*c*) Statically neutral system.

7.2.1 Static Stability

Consider a marble on a curved surface, such as a bowl. Imagine that the bowl is upright and the marble is resting inside, as shown in Fig. 7.6*a*. The marble is stationary; it is in a state of *equilibrium,* which means that the moments acting on the marble are zero. If the marble is now disturbed (moved to one side, as shown by the dotted circle in Fig. 7.6*a*) and then released, it will roll back toward the bottom of the bowl, that is, toward its original equilibrium position. Such a system is *statically stable*. In general, we can state that

> If the forces and moments on the body caused by a disturbance tend initially to return the body toward its equilibrium position, the body is statically stable. The body has positive static stability.

Now, imagine the bowl is upside down, with the marble at the crest, as shown in Fig. 7.6*b*. If the marble is placed precisely at the crest, the moments will be zero, and the marble will be in equilibrium. However, if the marble is now disturbed (as shown by the dotted circle in Fig. 7.6*b*), it will tend to roll down the side, away from its equilibrium position. Such a system is *statically unstable*. In general, we can state that

> If the forces and moments are such that the body continues to move *away* from its equilibrium position after being disturbed, the body is *statically unstable.* The body has *negative* static stability.

Finally, imagine the marble on a flat horizontal surface, as shown in Fig. 7.6*c*. Its moments are zero; it is in equilibrium. If the marble is now disturbed to another location, the moments will still be zero, and it will still be in equilibrium. Such a system is *neutrally stable*. This situation is rare in flight vehicles, and we will not be concerned with it here.

We emphasize that static stability (or the lack of it) deals with the *initial* tendency of a vehicle to return to equilibrium (or to diverge from equilibrium) after being disturbed. It says nothing about whether it ever reaches its equilibrium position, or how it gets there. Such matters are the realm of dynamic stability, as follows.

7.2.2 Dynamic Stability

Dynamic stability deals with the *time history* of the vehicle's motion after it initially responds to its static stability. For example, consider an airplane flying at an angle of attack α_e such that its moments about the center of gravity are zero. The airplane is therefore in equilibrium at α_e; in this situation, it is *trimmed,* and α_e is called the *trim angle of attack.* Now assume that the airplane is disturbed (say, by encountering a wind gust) to a new angle of attack α, as shown in Fig. 7.7. The airplane has been pitched through a *displacement* $\alpha - \alpha_e$. Now, let us observe the subsequent pitching motion after the airplane has been disturbed by the gust. We can describe this motion by plotting the instantaneous displacement versus time, as shown in Fig. 7.8. Here $\alpha - \alpha_e$ is given as a function of time t. At $t = 0$, the displacement is equal to that produced by the gust. If the airplane is statically stable, it will *initially* tend to move back toward its equilibrium position; that is, $\alpha - \alpha_e$ will initially decrease. Over a lapse of time, the vehicle may monotonically "home in" to its equilibrium position, as shown in Fig. 7.8*a*. Such motion is called *aperiodic.* Alternately, it may first overshoot the equilibrium position and approach α_e after a series of oscillations with decreasing amplitude, as shown in Fig. 7.8*b*. Such motion is described as *damped oscillations.* In both situations, Figs. 7.8*a* and 7.8*b*, the airplane eventually returns to its equilibrium

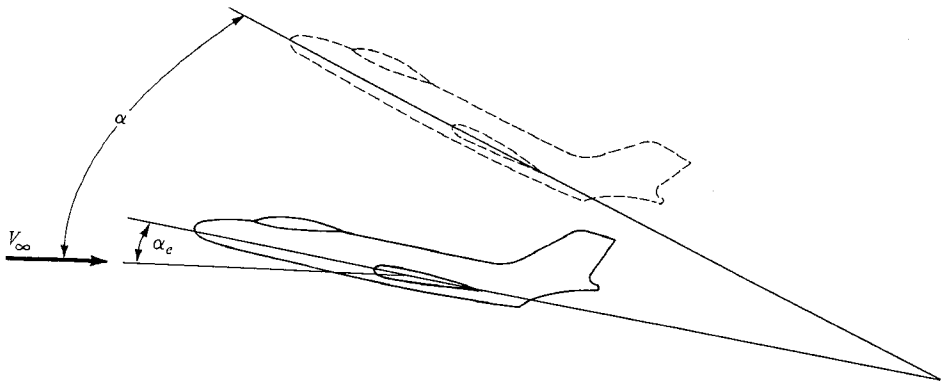

Figure 7.7 Disturbance from the equilibrium angle of attack.

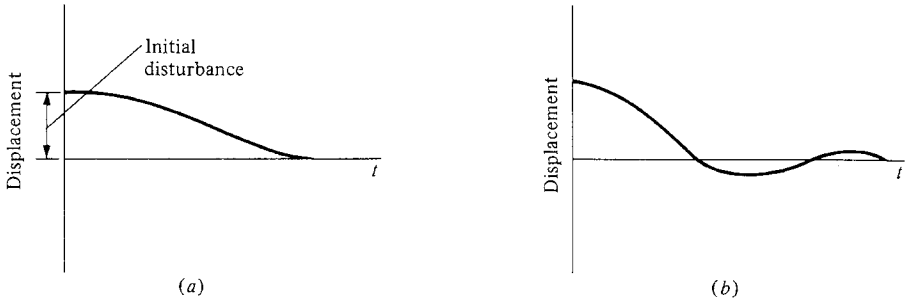

Figure 7.8 Examples of dynamic stability. (*a*) Aperiodic. (*b*) Damped oscillations.

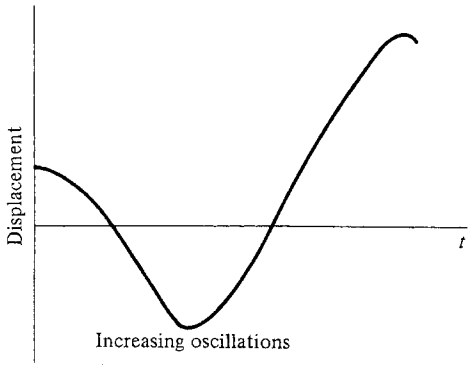

Figure 7.9 An example of dynamic instability.

position after some interval of time. These two situations are examples of *dynamic stability* in an airplane. Thus, we can state that

> A body is dynamically stable if, out of its own accord, it eventually returns to and remains at its equilibrium position over a period of time.

On the other hand, after initially responding to its static stability, the airplane may oscillate with increasing amplitude, as shown in Fig. 7.9. Here, the equilibrium position is never maintained for any period of time, and the airplane eventually diverges completely; the airplane in this case is *dynamically unstable* (even though it is statically stable). Also, it is theoretically possible for the airplane to pitch back and forth with constant-amplitude oscillations. This is an example of a *dynamically neutral* body; such a case is of little practical interest here.

It is important to observe from the preceding examples that a dynamically stable airplane must always be statically stable. However, static stability is *not* sufficient to ensure dynamic stability. Nevertheless, static stability is usually the first stability characteristic to be designed into an airplane. (There are some exceptions, to be discussed later.) Such considerations are of paramount importance in conventional airplanes, and therefore, most of this chapter will deal with

static stability and control. A study of dynamic stability, although of great importance, requires rather advanced analytical techniques beyond the scope of this book.

7.2.3 Control

The conventional control surfaces (elevators, ailerons, and rudder) on an airplane were discussed in Sec. 7.1 and sketched in Figs. 7.3 and 7.4. Their function is usually (1) to change the airplane from one equilibrium position to another and (2) to produce nonequilibrium accelerated motions such as maneuvers. The study of the *deflections* of the ailerons, elevators, and rudder necessary to make the airplane do what we want and of the amount of *force* that must be exerted by the pilot (or the hydraulic boost system) to deflect these controls is part of a discipline called *airplane control,* to be discussed later in this chapter.

7.2.4 Partial Derivative

Some physical definitions associated with stability and control have been given in Secs. 7.2.1 through 7.2.3. In addition, a mathematical definition, namely, that of the partial derivative, will be useful in the equations developed later, not only in this chapter but in our discussion of astronautics (Chap. 8) as well. For those readers having only a nodding acquaintance with calculus, hopefully this section will be self-explanatory; for those with a deeper calculus background, this should serve as a brief review.

Consider a function, say, $f(x)$, of a single variable x. The derivative of $f(x)$ is defined from elementary calculus as

$$\frac{df}{dx} \equiv \lim_{\Delta x \to 0} \left[\frac{f(x + \Delta x) - f(x)}{\Delta x} \right]$$

Physically, this limit represents the instantaneous rate of change of $f(x)$ with respect to x.

Now consider a function that depends on more than one variable, for example, the function $g(x, y, z)$, which depends on the three independent variables x, y, and z. Let x vary, while y and z are held constant. Then, the instantaneous rate of change of g with respect to x is given by

$$\frac{\partial g}{\partial x} \equiv \lim_{\Delta x \to 0} \left[\frac{g(x + \Delta x, y, z) - g(x, y, z)}{\Delta x} \right]$$

Here $\partial g / \partial x$ is the *partial derivative* of g with respect to x. Now let y vary, while holding x and z constant. Then, the instantaneous rate of change of g with respect to y is given by

$$\frac{\partial g}{\partial y} \equiv \lim_{\Delta y \to 0} \left[\frac{g(x, y + \Delta y, z) - g(x, y, z)}{\Delta y} \right]$$

Here, $\partial g/\partial y$ is the *partial derivative* of g with respect to y. An analogous definition holds for the partial derivative with respect to z, denoted by $\partial g/\partial z$.

In this book, we use the concept of the partial derivative as a definition only. The calculus of partial derivatives is essential to the advanced study of virtually any field of engineering, but such considerations are beyond the scope of this book.

EXAMPLE 7.1

If $g = x^2 + y^2 + z^2$, calculate $\partial g/\partial z$.

■ Solution

From the definition given in the preceding discussion, the partial derivative is taken with respect to z, holding x and y constant.

$$\frac{\partial g}{\partial z} = \frac{\partial (x^2 + y^2 + z^2)}{\partial z} = \frac{\partial x^2}{\partial z} + \frac{\partial y^2}{\partial z} + \frac{\partial z^2}{\partial z} = 0 + 0 + 2z = 2z$$

7.3 MOMENTS ON THE AIRPLANE

A study of stability and control is focused on moments: moments on the airplane and moments on the control surfaces. At this stage, it would be well for the reader to review the discussion of aerodynamically produced moments in Sec. 5.2. Recall that the pressure and shear stress distributions over a wing produce a pitching moment. This moment can be taken about any arbitrary point (the leading edge, the trailing edge, the quarter chord, etc.). However, there exists a particular point about which the moments are independent of the angle of attack. This point is defined as the *aerodynamic center* for the wing. The moment and its coefficient about the aerodynamic center are denoted by M_{ac} and $C_{M,ac}$, respectively, where $C_{M,ac} \equiv M_{ac}/(q_\infty Sc)$.

Reflecting again on Sec. 5.2, consider the force diagram of Fig. 5.5. Assume the wing is flying at zero lift; hence, F_1 and F_2 are equal and opposite forces. Thus, the moment established by these forces is a pure couple, which we know from elementary physics can be translated anywhere on the body at constant value. Therefore, at *zero lift*, $M_{ac} = M_{c/4} = M_{\text{any point}}$. In turn,

$$C_{M,ac} = (C_{M,c/4})_{L=0} = (C_{M,\text{any point}})_{L=0}$$

This says that the value of $C_{M,ac}$ (which is constant for angles of attack) can be obtained from the value of the moment coefficient about any point when the wing is at the zero-lift angle of attack $\alpha_{L=0}$. For this reason, M_{ac} is sometimes called the *zero-lift moment*.

The aerodynamic center is a useful concept for the study of stability and control. In fact, the force and moment system on a wing can be completely specified by the lift and drag acting through the aerodynamic center, plus the moment about the aerodynamic center, as sketched in Fig. 7.10. We adopt this convention for the remainder of this chapter.

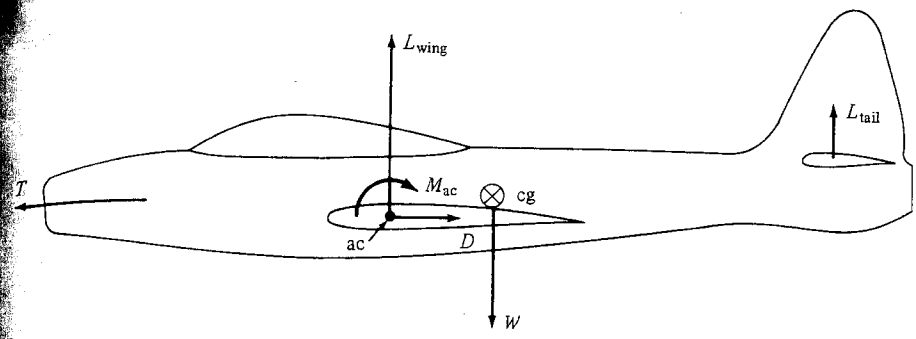

Figure 7.10 Contributions to the moment about the center of gravity of the airplane.

Now consider the complete airplane, as sketched in Fig. 7.10. Here we are most concerned with the pitching moment about the center of gravity of the airplane M_{cg}. Clearly, by examination of Fig. 7.10, M_{cg} is created by (1) L, D, and M_{ac} of the wing; (2) lift of the tail; (3) thrust; and (4) aerodynamic forces and moments on other parts of the airplane, such as the fuselage and engine nacelles. (Note that weight does not contribute, since it acts through the center of gravity.) These contributions to M_{cg} will be treated in detail later. The purpose of Fig. 7.10 is simply to illustrate the important conclusion that a moment does exist about the center of gravity of an airplane, and it is this moment that is fundamental to the stability and control of the airplane.

The moment coefficient about the center of gravity is defined as

$$C_{M,cg} = \frac{M_{cg}}{q_\infty Sc} \tag{7.1}$$

Combining the preceding concept with the discussion of Sec. 7.2, we find an airplane is in equilibrium (in pitch) when the moment about the center of gravity is zero; that is, when $M_{cg} = C_{M,cg} = 0$, the airplane is said to be *trimmed*.

7.4 ABSOLUTE ANGLE OF ATTACK

Continuing with our collection of tools to analyze stability and control, we consider a wing at an angle of attack such that lift is zero; that is, the wing is at the zero-lift angle of attack $\alpha_{L=0}$, as shown in Fig. 7.11*a*. With the wing in this orientation, draw a line through the trailing edge parallel to the relative wind V_∞. This line is defined as the *zero-lift line* for the airfoil. It is a fixed line; visualize it frozen into the geometry of the airfoil, as sketched in Fig. 7.11*a*. As discussed in Chap. 5, conventional cambered airfoils have slightly negative zero-lift angles; therefore, the zero-lift line lies slightly above the chord line, as shown (with overemphasis) in Fig. 7.11*a*.

Now consider the wing pitched to the geometric angle of attack α such that lift is generated, as shown in Fig. 7.11*b*. (Recall from Chap. 5 that the geometric angle of attack is the angle between the free-stream relative wind and the chord

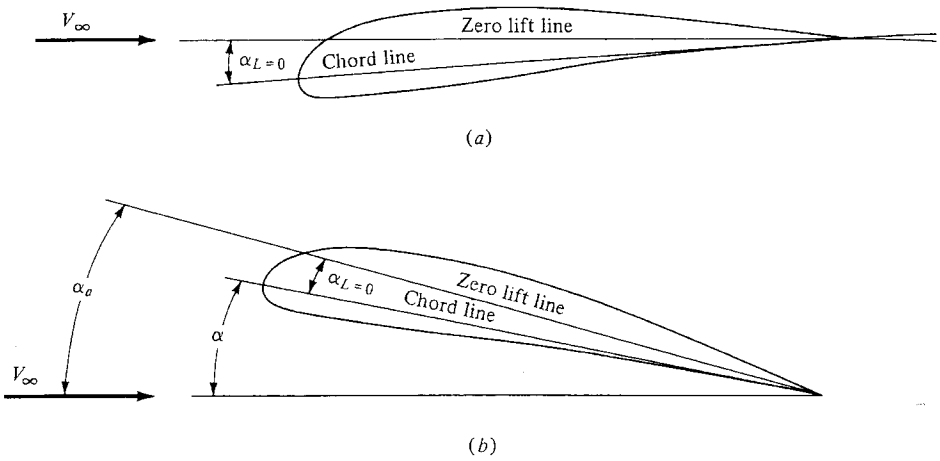

Figure 7.11 Illustration of the zero-lift line and absolute angle of attack. (*a*) No lift; (*b*) with lift.

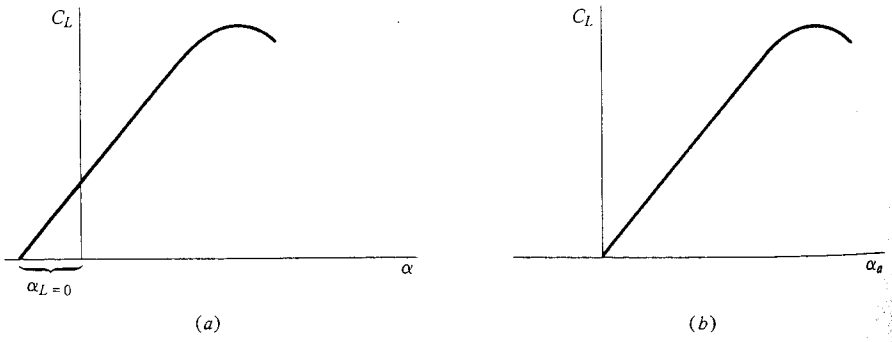

Figure 7.12 Lift coefficient versus (*a*) geometric angle of attack and (*b*) absolute angle of attack.

line.) In the same configuration, Fig. 7.11*b* demonstrates that the angle between the zero-lift line and the relative wind is equal to the sum of α and the absolute value of $\alpha_{L=0}$. This angle is defined as the *absolute angle of attack* α_a. From Fig. 7.11*b*, $\alpha_a = \alpha + \alpha_{L=0}$ (using $\alpha_{L=0}$ in an absolute sense). The geometry of Fig. 7.11*a* and 7.11*b* should be studied carefully until the concept of α_a is clearly understood.

The definition of the absolute angle of attack has a major advantage. When $\alpha_a = 0$, then $L = 0$, no matter what the camber of the airfoil. To further illustrate, consider the lift curves sketched in Fig. 7.12. The conventional plot (as discussed in detail in Chap. 5), C_L versus α, is shown in Fig. 7.12*a*. Here the lift curve does not go through the origin, and, of course, $\alpha_{L=0}$ is different for different airfoils. In contrast, when C_L is plotted versus α_a, as sketched in Fig. 7.12*b*, the curve always goes through the origin (by definition of α_a). The curve in

Fig. 7.12*b* is identical to that in Fig. 7.12*a*; only the abscissa has been translated by the value $\alpha_{L=0}$.

The use of α_a in lieu of α is common in studies of stability and control. We adopt this convention for the remainder of this chapter.

7.5 CRITERIA FOR LONGITUDINAL STATIC STABILITY

Static stability and control about all three axes shown in Fig. 7.2 are usually a necessity in the design of conventional airplanes. However, a complete description of all three types—lateral, longitudinal, and directional static stability and control (see Fig. 7.4)—is beyond the scope of this book. Rather, the intent here is to provide only the flavor of stability and control concepts, and to this end, only the airplane's longitudinal motion (pitching motion about the y axis) is considered in detail. This pitching motion is illustrated in Fig. 7.4*b*. It takes place in the plane of symmetry of the airplane. Longitudinal stability is also the most important static stability mode; in airplane design, wind tunnel testing, and flight research, it usually earns more attention than lateral or directional stability.

Consider a rigid airplane with fixed controls, for example, the elevator in some fixed position. Assume the airplane has been tested in a wind tunnel or free flight and that its variation of M_{cg} with angle of attack has been measured. This variation is illustrated in Fig. 7.13, where $C_{M,cg}$ is sketched versus α_a. For many conventional airplanes, the curve is nearly linear, as shown in Fig. 7.13. The value of $C_{M,cg}$ at zero lift (where $\alpha_a = 0$) is denoted by $C_{M,0}$. The value of α_a where $M_{cg} = 0$ is denoted by α_e; as stated in Sec. 7.3, this is the equilibrium, or trim, angle of attack.

Consider the airplane in steady, equilibrium flight at its trim angle of attack α_e, as shown in Fig. 7.14*a*. Suddenly, the airplane is disturbed by hitting a wind gust, and the angle of attack is momentarily changed. There are two possibilities: an increase or a decrease in α_a. If the airplane is pitched upward, as shown in Fig. 7.14*b*, then $\alpha_a > \alpha_e$. From Fig. 7.13, if $\alpha_a > \alpha_e$, the moment about the

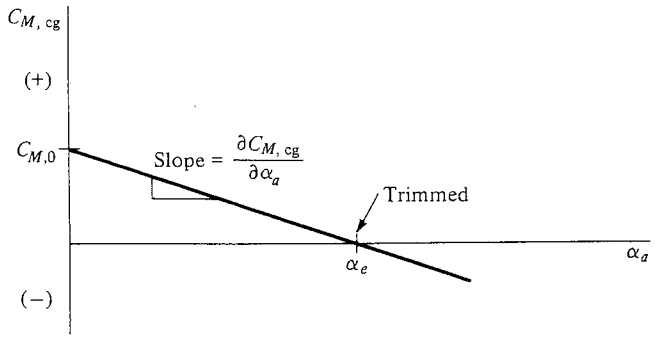

Figure 7.13 Moment coefficient curve with a negative slope.

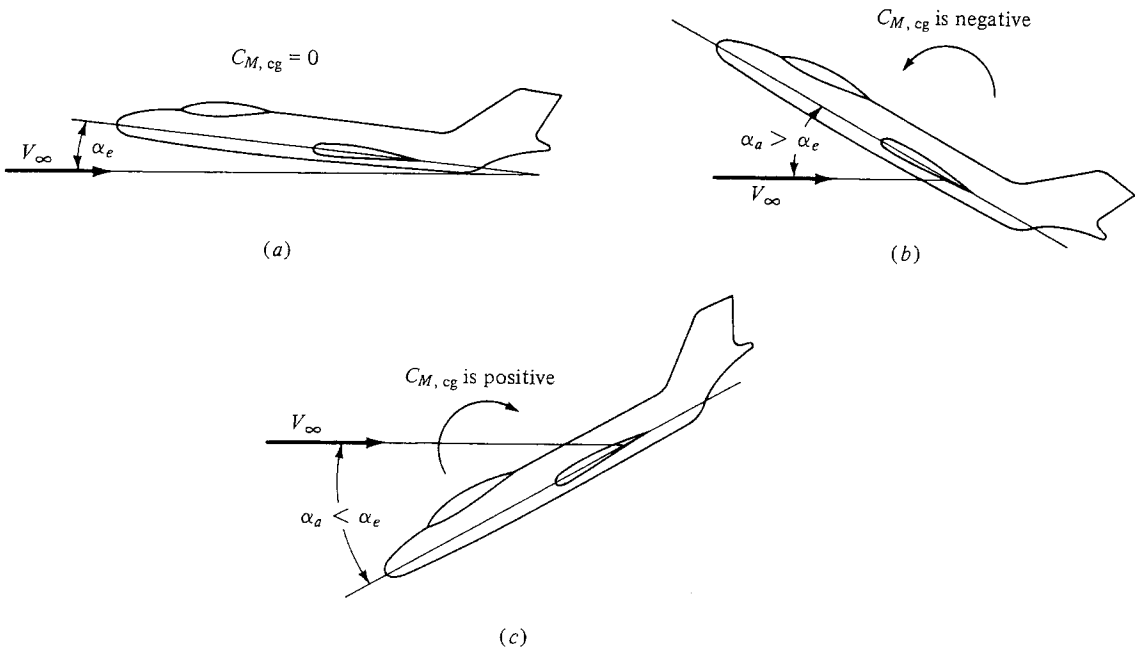

Figure 7.14 Illustration of static stability: (*a*) Equilibrium position (trimmed). (*b*) Pitched upward by disturbance. (*c*) Pitched downward by disturbance. In both (*b*) and (*c*), the airplane has the initial tendency to return to its equilibrium position.

center of gravity is negative. As discussed in Sec. 5.4, a negative moment (by convention) is counterclockwise, tending to pitch the nose downward. Hence, in Fig. 7.14*b*, the airplane will initially tend to move back toward its equilibrium position after being disturbed. On the other hand, if the plane is pitched downward by the gust, as shown in Fig. 7.14*c*, then $\alpha_a < \alpha_e$. From Fig. 7.13, the resulting moment about the center of gravity will be positive (clockwise) and will tend to pitch the nose upward. Thus, again we have the situation in which the airplane will initially tend to move back toward its equilibrium position after being disturbed. From Sec. 7.2, this is precisely the definition of static stability. Therefore, we conclude that an airplane that has a $C_{M,cg}$-versus-α_a variation like that shown in Fig. 7.13 is *statically stable*. Note from Fig. 7.13 that $C_{M,0}$ is positive and that the slope of the curve $\partial C_{M,cg}/\partial\alpha_a$ is negative. Here, the partial derivative, defined in Sec. 7.2.4, is used for the slope of the moment coefficient curve. This is because (as we shall see) $C_{M,cg}$ depends on a number of other variables in addition to α_a, and therefore it is mathematically proper to use $\partial C_{M,cg}/\partial\alpha_a$ rather than $dC_{M,cg}/d\alpha_a$ to represent the slope of the line in Fig. 7.13. As defined in Sec. 7.2.4, $\partial C_{M,cg}/\partial\alpha_a$ symbolizes the instantaneous rate of change of $C_{M,cg}$ with respect to α_a, with all other variables held constant.

Consider now a different airplane, with a measured $C_{M,cg}$ variation as shown in Fig. 7.15. Imagine the airplane is flying at its trim angle of attack α_e as shown

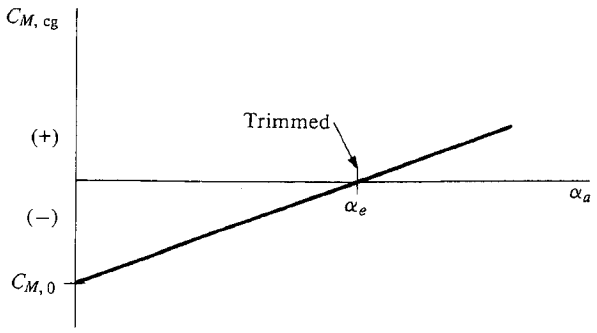

Figure 7.15 Moment coefficient curve with a positive slope.

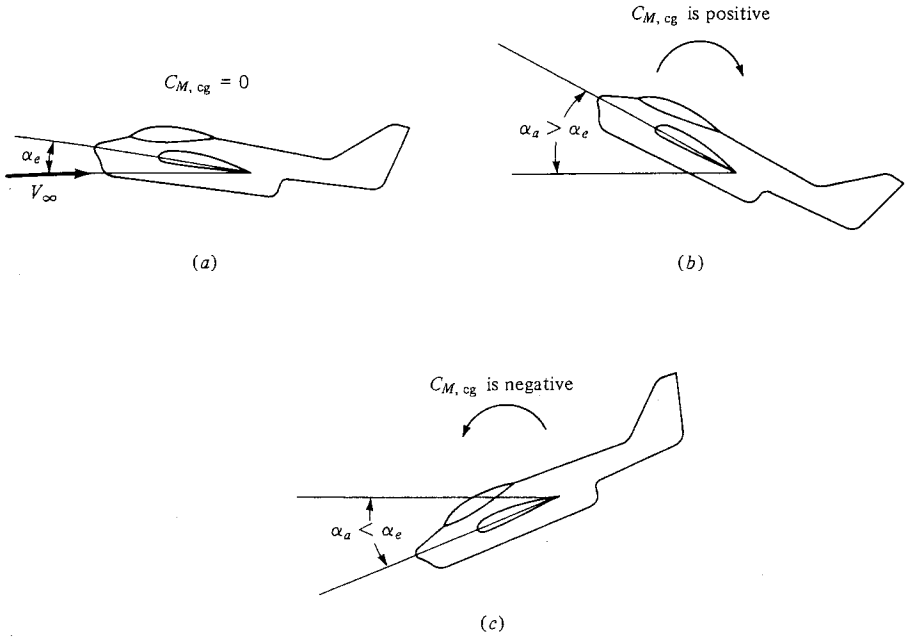

Figure 7.16 Illustration of static instability. (*a*) Equilibrium position (trimmed). (*b*) Pitched upward by disturbance. (*c*) Pitched downward by disturbance. In both (*b*) and (*c*), the airplane has the initial tendency to diverge farther away from its equilibrium position.

in Fig. 7.16*a*. If it is disturbed by a gust, pitching the nose upward, as shown in Fig. 7.16*b*, then $\alpha_a > \alpha_e$. From Fig. 7.15, this results in a positive (clockwise) moment, which tends to pitch the nose even farther away from its equilibrium position. Similarly, if the gust pitches the nose downward (Fig. 7.16*c*), a negative (counterclockwise) moment results, which also tends to pitch the nose farther away from its equilibrium position. Therefore, because the airplane always tends to diverge from equilibrium when disturbed, it is *statically unstable*. Note from Fig. 7.15 that $C_{M,0}$ is negative and $\partial C_{M,cg}/\partial \alpha_a$ is positive for this airplane.

For both airplanes, Figs. 7.13 and 7.15 show a positive value of α_e. Recall from Fig. 6.8 that an airplane moves through a range of angle of attack as it flies through its velocity range from V_{stall} (where α_a is the largest) to $V_{\max}$ (where α_a is the smallest). The value of α_e must fall within this flight range of angle of attack, or else the airplane cannot be trimmed for steady flight. (Remember that we are assuming a fixed elevator position: We are discussing stick-fixed stability.) When α_e does fall within this range, the airplane is *longitudinally balanced.*

From the preceding considerations, we conclude the following.

The necessary criteria for longitudinal balance and static stability are

1. $C_{M,0}$ must be positive.
2. $\partial C_{M,\text{cg}}/\partial \alpha_a$ must be negative.

That is, the $C_{M,\text{cg}}$ curve must look like Fig. 7.13.

Of course, implicit in this criteria is that α_e must also fall within the flight range of angle of attack for the airplane.

We are now in a position to explain why a conventional airplane has a horizontal tail (the horizontal stabilizer shown in Fig. 7.3). First, consider an ordinary wing (by itself) with a conventional airfoil, say an NACA 2412 section. Note from the airfoil data in App. D that the moment coefficient about aerodynamic center is negative. This is characteristic of all airfoils with positive camber. Now assume that the wing is at zero lift. In this case, the only moment on the wing is a pure couple, as explained in Sec. 7.3; hence, at zero lift, the moment about one point is equal to the moment about any other point. In particular,

$$C_{M,\text{ac}} = C_{M,\text{cg}} \qquad \text{for zero lift (wing only)} \tag{7.2}$$

On the other hand, examination of Fig. 7.13 shows that $C_{M,0}$ is, by definition, the moment coefficient about the center of gravity at zero lift (when $\alpha_a = 0$). Hence, from Eq. (7.2),

$$C_{M,0} = C_{M,\text{ac}} \qquad \text{wing only} \tag{7.3}$$

Equation (7.3) demonstrates that for a wing with positive camber ($C_{M,\text{ac}}$ negative), $C_{M,0}$ is also negative. Hence, such a wing by itself is *unbalanced.* To rectify this situation, a horizontal tail must be added to the airplane, as shown in Fig. 7.17*a* and 7.17*b*. If the tail is mounted behind the wing, as shown in Fig. 7.17*a*, and if it is inclined downward to produce a negative tail lift as shown, then a clockwise moment about the center of gravity will be created. If this clockwise moment is strong enough, then it will overcome the negative $C_{M,\text{ac}}$, and $C_{M,0}$ for the wing-tail combination will become positive. The airplane will then be balanced.

The arrangement shown in Fig. 7.17*a* is characteristic of most conventional airplanes. However, the tail can also be placed ahead of the wing, as shown in Fig. 7.17*b*; this is called a *canard configuration.* For a canard, the tail is inclined upward to produce a positive lift, hence creating a clockwise moment about the center of gravity. If this moment is strong enough, then $C_{M,0}$ for the wing-tail combination will become positive, and again the airplane will be balanced. Unfortunately, the forward-located tail of a canard interferes with the smooth aerodynamic flow over the wing. For this and other reasons, canard configurations

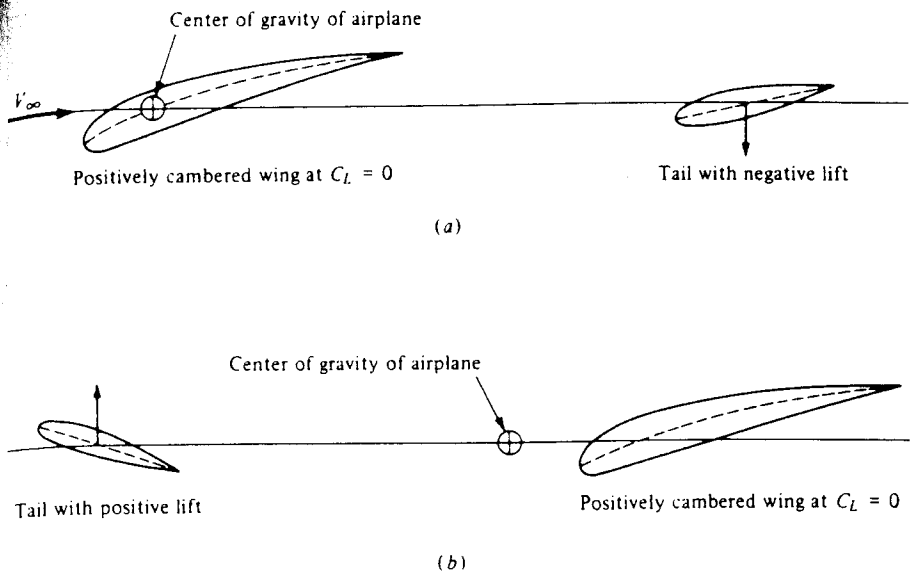

Figure 7.17 (*a*) Conventional wing-tail combination. The tail is set at such an angle as to produce negative lift, thus providing a positive $C_{M,0}$. (*b*) Canard wing-tail combination. The tail is set at such an angle as to produce positive lift, thus providing a positive $C_{M,0}$.

have not been popular. Of course, a notable exception were the *Wright Flyers,* which were canards. In fact, it was not until 1910 that the Wright brothers went to a conventional arrangement. Using the word *rudder* to mean elevator, Orville wrote to Wilbur in 1909 that "the difficulty in handling our machine is due to the rudder being in front, which makes it hard to keep on a level course. . . . I do not think it is necessary to lengthen the machine, but to simply put the rudder behind instead of before." Originally, the Wrights thought the forward-located elevator would help to protect them from the type of fatal crash encountered by Lilienthal. This rationale persisted until the design of their model B in 1910. Finally, a modern example of a canard is the North American XB-70, an experimental supersonic bomber developed for the Air Force in the 1960s. The canard surfaces ahead of the wing are clearly evident in the photograph shown in Fig. 7.18. In recent years, canards have come back on the aeronautical scene, for some high-performance military airplanes and special general aviation designs. The X-29 shown in Fig. 5.61 is a canard.

In retrospect, using essentially qualitative arguments based on physical reasoning and without resort to complicated mathematical formulas, we have developed some fundamental results for longitudinal static stability. Indeed, it is somewhat amazing how far our discussion has progressed on such a qualitative basis. However, we now turn to some quantitative questions. For a given airplane, how far should the wing and tail be separated in order to obtain stability? How large should the tail be made? How do we design for a desired trim angle α_e? These and other such questions are addressed in the remainder of this chapter.

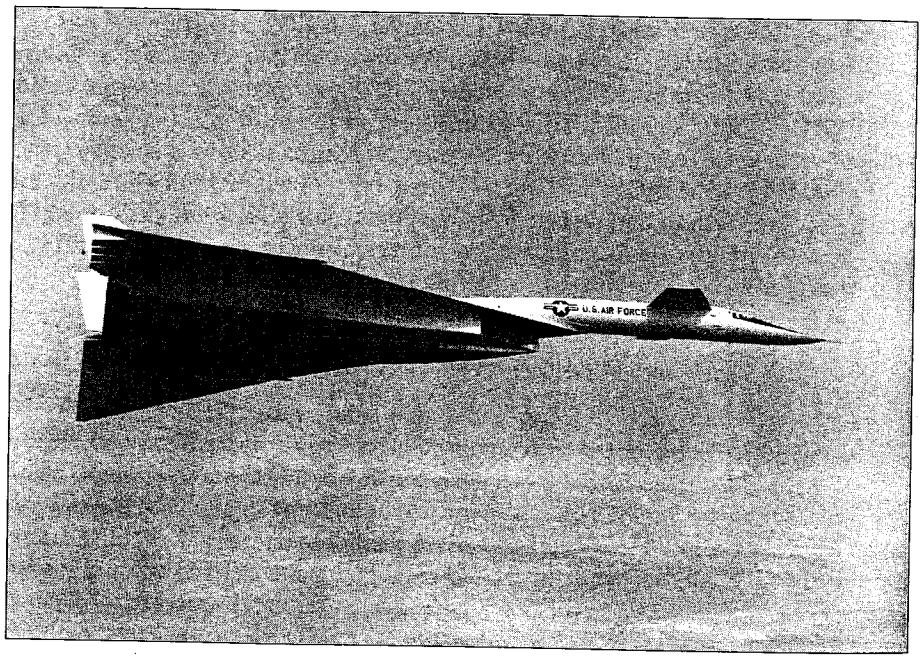

Figure 7.18 The North American XB-70. Note the canard surfaces immediately behind the cockpit.
(Source: *Rockwell International Corp.*)

7.6 QUANTITATIVE DISCUSSION: CONTRIBUTION OF THE WING TO M_{cg}

The calculation of moments about the center of gravity of the airplane M_{cg} is critical to a study of longitudinal static stability. The previous sections have already underscored this fact. Therefore, we now proceed to consider individually the contributions of the wing, fuselage, and tail to moments about the center of gravity of the airplane, in the end combining them to obtain the total M_{cg}.

Consider the forces and moments on the wing only, as shown in Fig. 7.19. Here the zero-lift line is drawn horizontally for convenience; hence, the relative wind is inclined at the angle α_w with respect to the zero-lift line, where α_w is the absolute angle of attack of the wing. Let c denote the mean zero-lift chord of the wing (the chord measured along the zero-lift line). The difference between the zero-lift chord and the geometric chord (as defined in Chap. 5) is usually insignificant and will be ignored here. The center of gravity for the airplane is located a distance hc behind the leading edge, and zc above the zero-lift line, as shown. Hence, h and z are coordinates of the center of gravity in fractions of chord length. The aerodynamic center is a distance $h_{ac_w}c$ from the leading edge. The moment of the wing about the aerodynamic center of the wing is denoted by M_{ac_w}, and the wing lift and drag are L_w and D_w, respectively, as shown.

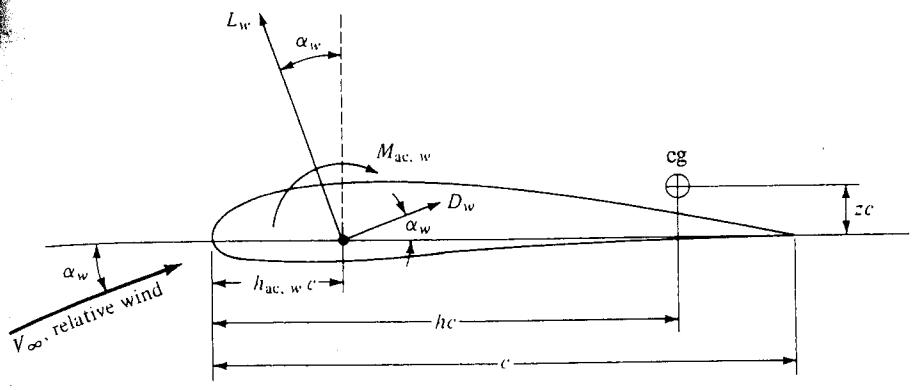

Figure 7.19 Airfoil nomenclature and geometry.

As usual, L_w and D_w are perpendicular and parallel, respectively, to the relative wind.

We wish to take moments about the center of gravity with pitch-up moments positive as usual. Clearly, from Fig. 7.19, L_w, D_w, and M_{ac_w}, all contribute to moments about the center of gravity. For convenience, split L_w and D_w into components perpendicular and parallel to the chord. Then, referring to Fig. 7.19, we find the moments about the center of gravity of the airplane due to the wing are

$$M_{cg_w} = M_{ac_w} + L_w \cos\alpha_w(hc - h_{ac_w}c) + D_w \sin\alpha_w(hc - h_{ac_w}c) + L_w \sin\alpha_w zc - D_w \cos\alpha_w zc \tag{7.4}$$

[Study Eq. (7.4) and Fig. 7.19 carefully, and make certain that you understand each term before progressing further.] For the normal-flight range of a conventional airplane, α_w is small; hence, the approximation is made that $\cos\alpha_w \approx 1$ and $\sin\alpha_w \approx \alpha_w$ (where α_w is in radians). Then Eq. (7.4) becomes

$$M_{cg_w} = M_{ac_w} + (L_w + D_w\alpha_w)(h - h_{ac_w})c + (L_w\alpha_w - D_w)zc \tag{7.5}$$

Dividing Eq. (7.5) by $q_\infty Sc$ and recalling that $C_M = M/(q_\infty Sc)$, we obtain the moment coefficient about the center of gravity as

$$C_{M,cg_w} = C_{M,ac_w} + (C_{L,w} + C_{D,w}\alpha_w)(h - h_{ac_w}) + (C_{L,w}\alpha_w - C_{D,w})z \tag{7.6}$$

For most airplanes, the center of gravity is located close to the zero-lift line; hence, z is usually small ($z \approx 0$) and will be neglected. Furthermore, α_w (in radians) is usually much less than unity, and $C_{D,w}$ is usually less than $C_{L,w}$; hence, the product $C_{D,w}\alpha_w$ is small in comparison to $C_{L,w}$. With these assumptions, Eq. (7.6) simplifies to

$$\boxed{C_{M,cg_w} = C_{M,ac_w} + C_{L,w}(h - h_{ac_w})} \tag{7.7}$$

Referring to Fig. 7.12*b*, we find $C_{L,w} = (dC_{L,w}/d\alpha)\alpha_w = a_w\alpha_w$, where a_w is the *lift slope of the wing*. Thus, Eq. (7.7) can be written as

$$C_{M,cg_w} = C_{M,ac_w} + a_w\alpha_w(h - h_{ac_w}) \tag{7.8}$$

Equations (7.7) and (7.8) give the contribution of the wing to moments about the center of gravity of the airplane, subject of course to the previously discussed assumptions. Closely examine Eqs. (7.7) and (7.8) along with Fig. 7.19. On a physical basis, they state the wing's contribution to M_{cg} is essentially due to two factors: the moment about the aerodynamic center M_{ac_w} and the lift acting through the moment arm $(h - h_{ac_w})c$.

These results are slightly modified if a fuselage is added to the wing. Consider a cigar-shaped body at an angle of attack to an airstream. This fuselage-type body experiences a moment about its aerodynamic center, plus some lift and drag due to the airflow around it. Now consider the fuselage and wing joined together: a *wing-body combination*. The airflow about this wing-body combination is different from that over the wing and body separately; aerodynamic interference occurs where the flow over the wing affects the fuselage flow, and vice versa. Due to this interference, the moment due to the wing-body combination is *not* simply the sum of the separate wing and fuselage moments. Similarly, the lift and drag of the wing-body combination are affected by aerodynamic interference. Such interference effects are extremely difficult to predict theoretically. Consequently, the lift, drag, and moments of a wing-body combination are usually obtained from wind tunnel measurements. Let $C_{L_{wb}}$ and $C_{M,ac_{wb}}$ be the lift coefficient and moment coefficient about the aerodynamic center, respectively, for the wing-body combination. Analogous to Eqs. (7.7) and (7.8) for the wing only, the contribution of the wing-body combination to M_{cg} is

$$C_{M,cg_{wb}} = C_{M,ac_{wb}} + C_{L_{wb}}(h - h_{ac_{wb}}) \tag{7.9}$$

$$C_{M,cg_{wb}} = C_{M,ac_{wb}} + a_{wb}\alpha_{wb}(h - h_{ac_{wb}}) \tag{7.10}$$

where a_{wb} and α_{wb} are the slope of the lift curve and absolute angle of attack, respectively, for the wing-body combination. In general, adding a fuselage to a wing shifts the aerodynamic center forward, increases the lift curve slope, and contributes a negative increment to the moment about the aerodynamic center. We emphasize again that the aerodynamic coefficients in Eqs. (7.9) and (7.10) are almost always obtained from wind tunnel data.

EXAMPLE 7.2

For a given wing-body combination, the aerodynamic center lies 0.05 chord length ahead of the center of gravity. The moment coefficient about the aerodynamic center is −0.016. If the lift coefficient is 0.45, calculate the moment coefficient about the center of gravity.

■ Solution

From Eq. (7.9),

$$C_{M,cg_{wb}} = C_{M,ac_{wb}} + C_{L_{wb}}(h - h_{ac_{wb}})$$

where
$$h - h_{ac_{wb}} = 0.05$$
$$C_{L_{wb}} = 0.45$$
$$C_{M,ac_{wb}} = -0.016$$

Thus,
$$C_{M,cg_{wb}} = -0.016 + 0.45(0.05) = \boxed{0.0065}$$

EXAMPLE 7.3

A wing-body model is tested in a subsonic wind tunnel. The lift is found to be zero at a geometric angle of attack $\alpha = -1.5°$. At $\alpha = 5°$, the lift coefficient is measured as 0.52. Also, at $\alpha = 1.0°$ and 7.88°, the moment coefficients about the center of gravity are measured as −0.01 and 0.05, respectively. The center of gravity is located at $0.35c$. Calculate the location of the aerodynamic center and the value of $C_{M,ac_{wb}}$.

■ Solution

First, calculate the lift slope:

$$a_{wb} \equiv \frac{dC_L}{d\alpha} = \frac{0.52 - 0}{5 - (-1.5)} = \frac{0.52}{6.5} = 0.08 \text{ per degree}$$

Write Eq. (7.10),

$$C_{M,cg_{wb}} = C_{M,ac_{wb}} + a_{wb}\alpha_{wb}(h - h_{ac_{wb}})$$

evaluated at $\alpha = 1.0°$ [remember that α is the geometric angle of attack, whereas in Eq. (7.10), α_{wb} is the absolute angle of attack]:

$$-0.01 = C_{M,ac_{wb}} + 0.08(1 + 1.5)(h - h_{ac_{wb}})$$

Then evaluate it at $\alpha = 7.88°$:

$$0.05 = C_{M,ac_{wb}} + 0.08(7.88 + 1.5)(h - h_{ac_{wb}})$$

The preceding two equations have two unknowns, $C_{M,ac_{wb}}$ and $h - h_{ac_{wb}}$. They can be solved simultaneously.

Subtracting the second equation from the first, we get

$$-0.06 = 0 - 0.55(h - h_{ac_{wb}})$$
$$h - h_{ac_{wb}} = \frac{-0.06}{-0.55} = 0.11$$

The value of h is given: $h = 0.35$. Thus,

$$h_{ac_{wb}} = 0.35 - 0.11 = \boxed{0.24}$$

In turn,
$$-0.01 = C_{M,ac_{wb}} + 0.08(1 + 1.5)(0.11)$$
$$C_{M,ac_{wb}} = \boxed{-0.032}$$

7.7 CONTRIBUTION OF THE TAIL TO M_{cg}

An analysis of moments due to an isolated tail taken independently of the airplane would be the same as that given for the isolated wing above. However, in real life, the tail is obviously connected to the airplane itself; it is not isolated. Moreover, the tail is generally mounted behind the wing; hence, it feels the wake of the airflow over the wing. As a result, there are two interference effects that influence the tail aerodynamics:

1. The airflow at the tail is deflected downward by the *downwash* due to the finite wing (see Secs. 5.13 and 5.14); that is, the relative wind seen by the tail is not in the same direction as the relative wind V_∞ seen by the wing.
2. Because of the retarding force of skin friction and pressure drag over the wing, the airflow reaching the tail has been slowed. Therefore, the velocity of the relative wind seen by the tail is less than V_∞. In turn, the dynamic pressure seen by the tail is less than q_∞.

These effects are illustrated in Fig. 7.20. Here V_∞ is the relative wind as seen by the wing, and V' is the relative wind at the tail, inclined below V_∞ by the downwash angle ε. The tail lift L_t and drag D_t are (by definition) perpendicular and parallel, respectively, to V'. In contrast, the lift and drag of the complete airplane are always (by definition) perpendicular and parallel, respectively, to V_∞. Therefore, considering components of L_t and D_t perpendicular to V_∞, we demonstrate in Fig. 7.20 that the tail contribution to the total airplane lift is $L_t \cos \varepsilon - D_t \sin \varepsilon$. In many cases, ε is very small, and thus $L_t \cos \varepsilon - D_t \sin \varepsilon \approx L_t$. Hence, for all practical purposes, it is sufficient to add the tail lift directly to the wing-body lift to obtain the lift of the complete airplane.

Consider the tail in relation to the wing-body zero-lift line, as illustrated in Fig. 7.21. It is useful to pause and study this figure. The wing-body combination is at an absolute angle of attack α_{wb}. The tail is twisted downward to provide a positive $C_{M,0}$, as discussed at the end of Sec. 7.5. Thus the zero-lift line of the tail is intentionally inclined to the zero-lift line of the wing-body combination at the

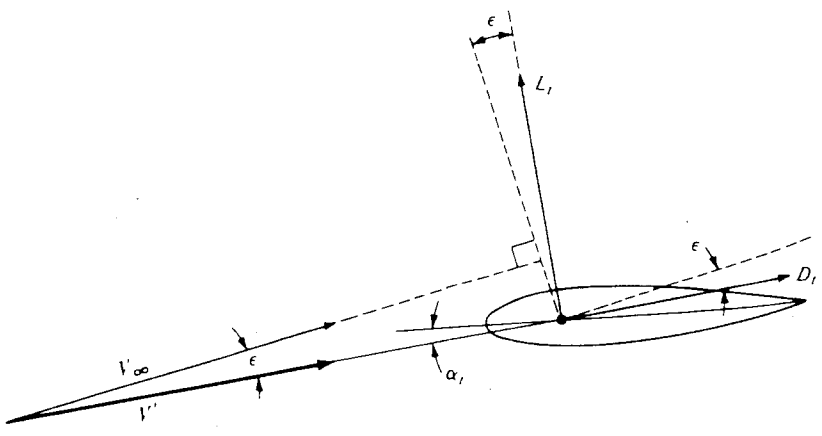

Figure 7.20 Flow and force diagram in the vicinity of the tail.

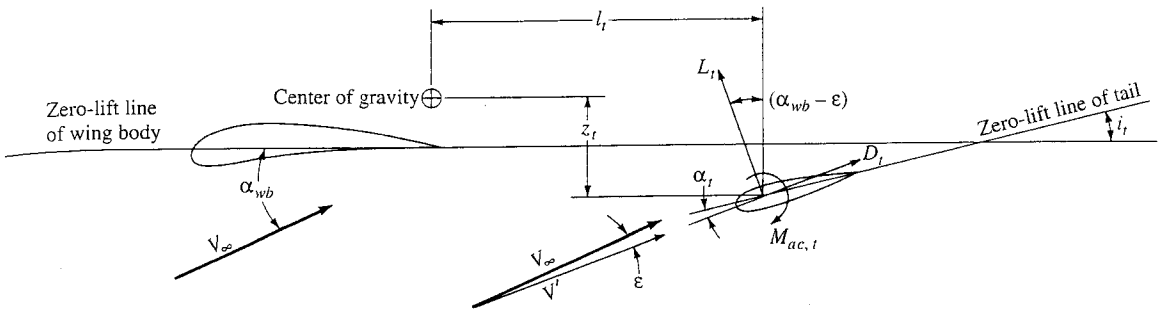

Figure 7.21 Geometry of wing-tail combination.

tail-setting angle i_t. (The airfoil section of the tail is generally symmetric, for which the tail zero-lift line and the tail chord line are the same.) The absolute angle of attack of the tail α_t is measured between the local relative wind V' and the tail zero-lift line. The tail has an aerodynamic center, about which there is a moment M_{ac_t} and through which L_t and D_t act perpendicular and parallel, respectively, to V'. As before, V' is inclined below V_∞ by the downwash angle ε; hence, L_t makes an angle $\alpha_{wb} - \varepsilon$ with the vertical. The tail aerodynamic center is located a distance l_t behind and z_t below the center of gravity of the airplane. Make certain to carefully study the geometry shown in Fig. 7.21; it is fundamental to the derivation that follows.

Split L_t and D_t into their vertical components $L_t \cos(\alpha_{wb} - \varepsilon)$ and $D_t \sin(\alpha_{wb} - \varepsilon)$ and their horizontal components $L_t \sin(\alpha_{wb} - \varepsilon)$ and $D_t \cos(\alpha_{wb} - \varepsilon)$. By inspection of Fig. 7.21, the sum of moments about the center of gravity due to L_t, D_t, and M_{ac_t} of the tail is

$$M_{cg_t} = -l_t[L_t \cos(\alpha_{wb} - \varepsilon) + D_t \sin(\alpha_{wb} - \varepsilon)] + z_t L_t \sin(\alpha_{wb} - \varepsilon) - z_t D_t \cos(\alpha_{wb} - \varepsilon) + M_{ac_t} \tag{7.11}$$

Here, M_{cg_t} denotes the contribution to moments about the airplane's center of gravity due to the horizontal tail.

In Eq. (7.11), the first term on the right-hand side, $l_t L_t \cos(\alpha_{wb} - \varepsilon)$, is by far the largest in magnitude. In fact, for conventional airplanes, the following simplifications are reasonable:

1. $z_t \ll l_t$.
2. $D_t \ll L_t$.
3. The angle $\alpha_{wb} - \varepsilon$ is small; hence, $\sin(\alpha_{wb} - \varepsilon) \approx 0$ and $\cos(\alpha_{wb} - \varepsilon) \approx 1$.
4. M_{ac_t} is small in magnitude.

With the preceding approximations, which are based on experience, Eq. (7.11) is dramatically simplified to

$$M_{cg_t} = -l_t L_t \tag{7.12}$$

Define the *tail lift coefficient,* based on free-stream dynamic pressure $q_\infty = \frac{1}{2}\rho_\infty V_\infty^2$ and the tail planform area S_t, as

$$C_{L,t} = \frac{L_t}{q_\infty S_t} \tag{7.13}$$

Combining Eqs. (7.12) and (7.13), we obtain

$$M_{\text{cg},t} = -l_t q_\infty S_t C_{L,t} \tag{7.14}$$

Dividing Eq. (7.14) by $q_\infty Sc$, where c is the wing chord and S is the wing planform area, gives

$$\frac{M_{\text{cg},t}}{q_\infty Sc} \equiv C_{M,\text{cg},t} = -\frac{l_t S_t}{cS} C_{L,t} \tag{7.15}$$

Examining the right-hand side of Eq. (7.15), we note that $l_t S_t$ is a *volume* characteristic of the size and location of the tail and that cS is a *volume* characteristic of the size of the wing. The ratio of these two volumes is called the *tail volume ratio* V_H, where

$$V_H \equiv \frac{l_t S_t}{cS} \tag{7.16}$$

Thus, Eq. (7.15) becomes

$$\boxed{C_{M,\text{cg},t} = -V_H C_{L,t}} \tag{7.17}$$

The simple relation in Eq. (7.17) gives the total contribution of the tail to moments about the airplane's center of gravity. With the preceding simplifications and by referring to Fig. 7.21, Eqs. (7.12) and (7.17) say that the moment is equal to tail lift operating through the moment arm l_t.

It will be useful to couch Eq. (7.17) in terms of angle of attack, as was done in Eq. (7.10) for the wing-body combination. Keep in mind that the stability criterion in Fig. 7.13 involves $\partial C_{M,\text{cg}}/\partial \alpha_a$; hence, equations in terms of α_a are directly useful. Specifically, referring to the geometry of Fig. 7.21, we see that the angle of attack of the tail is

$$\alpha_t = \alpha_{\text{wb}} - i_t - \varepsilon \tag{7.18}$$

Let a_t denote the lift slope of the tail. Thus, from Eq. (7.18),

$$C_{L,t} = a_t \alpha_t = a_t(\alpha_{\text{wb}} - i_t - \varepsilon) \tag{7.19}$$

The downwash angle ε is difficult to predict theoretically and is usually obtained from experiment. It can be written as

$$\varepsilon = \varepsilon_0 + \frac{\partial \varepsilon}{\partial \alpha} \alpha_{\text{wb}} \tag{7.20}$$

where ε_0 is the downwash angle when the wing-body combination is at zero lift. Both ε_0 and $\partial \varepsilon/\partial \alpha$ are usually obtained from wind tunnel data. Thus, combining Eqs. (7.19) and (7.20) yields

$$C_{L,t} = a_t \alpha_{\text{wb}} \left(1 - \frac{\partial \varepsilon}{\partial \alpha}\right) - a_t(i_t + \varepsilon_0) \tag{7.21}$$

Substituting Eq. (7.21) into (7.17), we obtain

$$\boxed{C_{M,\text{cg},t} = -a_t V_H \alpha_{\text{wb}} \left(1 - \frac{\partial \varepsilon}{\partial \alpha}\right) + a_t V_H (\varepsilon_0 + i_t)} \tag{7.22}$$

Equation (7.22), although lengthier than Eq. (7.17), contains the explicit dependence on angle of attack and will be useful for our subsequent discussions.

7.8 TOTAL PITCHING MOMENT ABOUT THE CENTER OF GRAVITY

Consider the airplane as a whole. The total M_{cg} is due to the contribution of the wing-body combination plus that of the tail:

$$C_{M,cg} = C_{M,cg_{wb}} + C_{M,cg_t} \tag{7.23}$$

Here, $C_{M,cg}$ is the total moment coefficient about the center of gravity for the complete airplane. Substituting Eqs. (7.9) and (7.17) into (7.23), we have

$$\boxed{C_{M,cg} = C_{M,ac_{wb}} + C_{L_{wb}}(h - h_{ac_{wb}}) - V_H C_{L,t}} \tag{7.24}$$

In terms of angle of attack, an alternate expression can be obtained by substituting Eqs. (7.10) and (7.22) into Eq. (7.23):

$$\boxed{C_{M,cg} = C_{M,ac_{wb}} + a_{wb}\alpha_{wb}\left[h - h_{ac_{wb}} - V_H \frac{a_t}{a_{wb}}\left(1 - \frac{\partial \varepsilon}{\partial \alpha}\right)\right] + V_H a_t (i_t + \varepsilon_0)} \tag{7.25}$$

The angle of attack needs further clarification. Referring again to Fig. 7.13, we find the moment coefficient curve is usually obtained from wind tunnel data, preferably on a model of the complete airplane. Hence, α_a in Fig. 7.13 should be interpreted as the absolute angle of attack referenced to the zero-lift line of the *complete airplane,* which is not necessarily the same as the zero-lift line for the wing-body combination. This comparison is sketched in Fig. 7.22. However, for many conventional aircraft, the difference is small. Therefore, in the remainder of this chapter, we assume the two zero-lift lines in Fig. 7.22 to be the same.

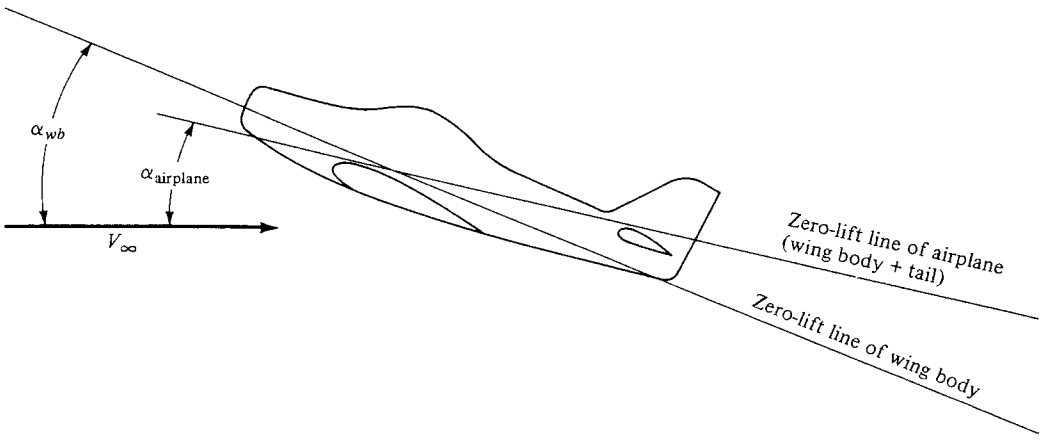

Figure 7.22 Zero-lift line of the wing-body combination compared with that of the complete airplane.

Thus, α_{wb} becomes the angle of attack of the complete airplane α_a. Consistent with this assumption, the total lift of the airplane is due to the wing-body combination, with the tail lift neglected. Hence, $C_{L_{wb}} = C_L$ and the lift slope $a_{wb} = a$, where C_L and a are for the complete airplane. With these interpretations, Eq. (7.25) can be rewritten as

$$\boxed{C_{M,cg} = C_{M,ac_{wb}} + a\alpha_a \left[h - h_{ac_{wb}} - V_H \frac{a_t}{a} \left(1 - \frac{\partial \varepsilon}{\partial \alpha} \right) \right] + V_H a_t (i_t + \varepsilon_0)} \tag{7.26}$$

Equation (7.26) is the same as Eq. (7.25), except that the subscript wb on some terms has been dropped in deference to properties for the whole airplane.

EXAMPLE 7.4

Consider the wing-body model in Example 7.3. The area and chord of the wing are 0.1 m^2 and 0.1 m, respectively. Now assume that a horizontal tail is added to this model. The distance from the airplane's center of gravity to the tail's aerodynamic center is 0.17 m, the tail area is 0.02 m^2, the tail-setting angle is 2.7°, the tail lift slope is 0.1 per degree, and from experimental measurement, $\varepsilon_0 = 0$ and $\partial\varepsilon/\partial\alpha = 0.35$. If $\alpha = 7.88°$, calculate $C_{M,cg}$ for the airplane model.

■ **Solution**

From Eq. (7.26),

$$C_{M,cg} = C_{M,ac_{wb}} + a\alpha_a \left[h - h_{ac_{wb}} - V_H \frac{a_t}{a} \left(1 - \frac{\partial \varepsilon}{\partial \alpha} \right) \right] + V_H a_t (i_t + \varepsilon_0)$$

where

$C_{M,ac_{wb}} = -0.032$ (from Example 7.3)

$a = 0.08$ (from Example 7.3)

$\alpha_a = 7.88 + 1.5 = 9.38°$ (from Example 7.3)

$h - h_{ac_{wb}} = 0.11$ (from Example 7.3)

$$V_H = \frac{l_t S_t}{cS} = \frac{0.17(0.02)}{0.1(0.1)} = 0.34$$

$a_t = 0.1$ per degree

$$\frac{\partial \varepsilon}{\partial \alpha} = 0.35$$

$i_t = 2.7°$

$\varepsilon_0 = 0$

Thus,

$$C_{M,cg} = -0.032 + 0.08(9.38) \left[0.11 - 0.34 \left(\frac{0.1}{0.08} \right) (1 - 0.35) \right] + 0.34(0.1)(2.7 + 0)$$

$$= -0.032 - 0.125 + 0.092 = \boxed{-0.065}$$

7.9 EQUATIONS FOR LONGITUDINAL STATIC STABILITY

The criteria necessary for longitudinal balance and static stability were developed in Sec. 7.5: they are (1) $C_{M,0}$ must be positive and (2) $\partial C_{M,cg}/\partial \alpha_a$ must be negative, both conditions with the implicit assumption that α_e falls within the practical flight range of angle of attack; that is, the moment coefficient curve must be similar to that sketched in Fig. 7.13. In turn, the ensuing sections developed a quantitative formalism for static stability culminating in Eq. (7.26) for $C_{M,cg}$. The purpose of this section is to combine the preceding results to obtain formulas for the direct calculation of $C_{M,0}$ and $\partial C_{M,cg}/\partial \alpha_a$. In this manner, we will be able to make a quantitative assessment of the longitudinal static stability of a given airplane, as well as point out some basic philosophy of airplane design.

Recall that, by definition, $C_{M,0}$ is the value of $C_{M,cg}$ when $\alpha_a = 0$, that is, when the lift is zero. Substituting $\alpha_a = 0$ into Eq. (7.26), we directly obtain

$$\boxed{C_{M,0} \equiv (C_{M,cg})_{L=0} = C_{M,ac_{wb}} + V_H a_t (i_t + \varepsilon_0)} \tag{7.27}$$

Examine Eq. (7.27). We know that $C_{M,0}$ must be positive in order to balance the airplane. However, the previous sections have pointed out that $C_{M,ac_{wb}}$ is negative for conventional airplanes. Therefore, $V_H a_t (i_t + \varepsilon_0)$ must be positive and large enough to more than counterbalance the negative $C_{M,ac}$. Both V_H and a_t are positive quantities, and ε_0 is usually so small that it exerts only a minor effect. Thus, i_t *must be a positive quantity.* This verifies our previous physical arguments that the tail must be set at an angle relative to the wing in the manner shown in Figs. 7.17*a* and 7.21. This allows the tail to generate enough negative lift to produce a positive $C_{M,0}$.

Consider now the slope of the moment coefficient curve. Differentiating Eq. (7.26) with respect to α_a, we obtain

$$\boxed{\frac{\partial C_{M,cg}}{\partial \alpha_a} = a\left[h - h_{ac_{wb}} - V_H \frac{a_t}{a}\left(1 - \frac{\partial \varepsilon}{\partial \alpha}\right)\right]} \tag{7.28}$$

This equation clearly shows the powerful influence of the location h of the center of gravity and the tail volume ratio V_H in determining longitudinal static stability.

Equations (7.27) and (7.28) allow us to check the static stability of a given airplane, assuming we have some wind tunnel data for a, a_t, $C_{M,ac_{wb}}$, ε_0, and $\partial \varepsilon/\partial \alpha$. They also establish a certain philosophy in the design of an airplane. For example, consider an airplane where the location h of the center of gravity is essentially dictated by payload or other mission requirements. Then the desired amount of static stability can be obtained simply by designing V_H large enough, via Eq. (7.28). Once V_H is fixed in this manner, then the desired $C_{M,0}$ (or the desired α_e) can be obtained by designing i_t appropriately, via Eq. (7.27). Thus, the values of $C_{M,0}$ and $\partial C_{M,cg}/\partial \alpha_a$ basically dictate the design values of i_t and V_H, respectively (for a fixed center-of-gravity location).

EXAMPLE 7.5

Consider the wing-body-tail wind tunnel model of Example 7.4. Does this model have longitudinal static stability and balance?

■ **Solution**

From Eq. (7.28),

$$\frac{\partial C_{M,\text{cg}}}{\partial \alpha_a} = a\left[h - h_{\text{ac}_{\text{wb}}} - V_H \frac{a_t}{a}\left(1 - \frac{\partial \varepsilon}{\partial \alpha}\right)\right]$$

where, from Examples 7.3 and 7.4,

$$a = 0.08$$
$$h - h_{\text{ac}_{\text{wb}}} = 0.11$$
$$V_H = 0.34$$
$$a_t = 0.1 \text{ per degree}$$
$$\frac{\partial \varepsilon}{\partial \alpha} = 0.35$$

Thus, $$\frac{\partial C_{M,\text{cg}}}{\partial \alpha_a} = 0.08\left[0.11 - 0.34\frac{0.1}{0.08}(1 - 0.35)\right] = \boxed{-0.0133}$$

The slope of the moment coefficient curve is negative; hence, the airplane model is statically stable.

However, is the model longitudinally balanced? To answer this, we must find $C_{M,0}$, which in combination with the preceding result for $\partial C_{M,\text{cg}}/\partial \alpha$ will yield the equilibrium angle of attack α_e. From Eq. (7.27),

$$C_{M,0} = C_{M,\text{ac}_{\text{wb}}} + V_H a_t (i_t + \varepsilon_0)$$

where from Examples 7.3 and 7.4,

$$C_{M,\text{ac}_{\text{wb}}} = -0.032$$
$$i_t = 2.7°$$

Thus, $$C_{M,0} = -0.032 + 0.34(0.1)(2.7) = 0.06$$

From Fig. 7.13, the equilibrium angle of attack is obtained from

$$0 = 0.06 - 0.0133\alpha_e$$

Thus, $$\alpha_e = 4.5°$$

Clearly, this angle of attack falls within the reasonable flight range. Therefore, the airplane is longitudinally balanced as well as statically stable.

7.10 NEUTRAL POINT

Consider the situation where the location h of the center of gravity is allowed to move, with everything else remaining fixed. In fact, Eq. (7.28) indicates that static stability is a strong function of h. Indeed, the value of $\partial C_{M,\text{cg}}/\partial \alpha_a$ can always be made negative by properly locating the center of gravity. In the same vein, there is one specific location of the center of gravity such that $\partial C_{M,\text{cg}}/\partial \alpha_a = 0$. The value of h when this condition holds is defined as the *neutral point,* denoted by h_n. When $h = h_n$, the slope of the moment coefficient curve is zero, as illustrated in Fig. 7.23.

The location of the neutral point is readily obtained from Eq. (7.28) by setting $h = h_n$ and $\partial C_{M,\text{cg}}/\partial \alpha_a = 0$, as follows.

$$0 = a\left[h_n - h_{\text{ac}_{\text{wb}}} - V_H \frac{a_t}{a}\left(1 - \frac{\partial \varepsilon}{\partial \alpha}\right)\right] \tag{7.29}$$

Solving Eq. (7.29) for h_n, we have

$$\boxed{h_n = h_{\text{ac}_{\text{wb}}} + V_H \frac{a_t}{a}\left(1 - \frac{\partial \varepsilon}{\partial \alpha}\right)} \tag{7.30}$$

Examine Eq. (7.30). The quantities on the right-hand side are, for all practical purposes, established by the design configuration of the airplane. Thus, for a *given* airplane design, the neutral point is a *fixed quantity,* that is, a point that is frozen somewhere on the airplane. It is quite independent of the actual location h of the center of gravity.

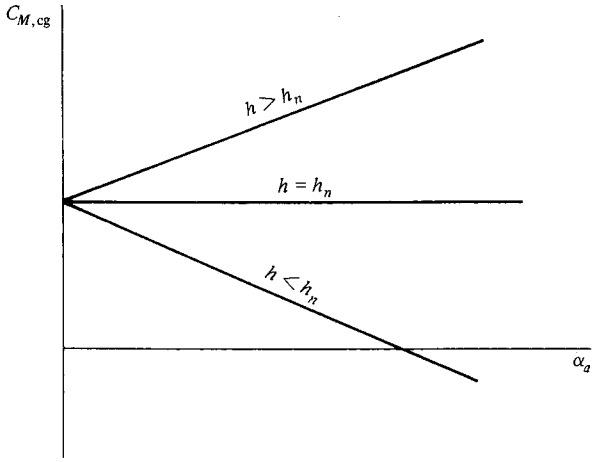

Figure 7.23 Effect of the location of the center of gravity, relative to the neutral point, on static stability.

The concept of the neutral point is introduced as an alternative stability criterion. For example, inspection of Eqs. (7.28) and (7.30) shows that $\partial C_{M,\text{cg}}/\partial \alpha_a$ is negative, zero, or positive depending on whether h is less than, equal to, or greater than h_n. These situations are sketched in Fig. 7.23. Remember that h is measured from the leading edge of the wing, as shown in Fig. 7.19. Hence, $h < h_n$ means that the center-of-gravity location is *forward* of the neutral point. Thus, an alternative stability criterion is as follows:

> For longitudinal static stability, the position of the center of gravity must always be forward of the neutral point.

Recall that the definition of the aerodynamic center for a wing is that point about which moments are independent of the angle of attack. This concept can now be extrapolated to the whole airplane by considering again Fig. 7.23. Clearly, when $h = h_n$, $C_{M,\text{cg}}$ is independent of the angle of attack. Therefore, the neutral point might be considered the aerodynamic center of the complete airplane.

Again examining Eq. (7.30), we see that the tail strongly influences the location of the neutral point. *By proper selection of the tail parameters, principally V_H, h_n can be located at will by the designer.*

EXAMPLE 7.6

For the wind tunnel model of Examples 7.3 to 7.5, calculate the neutral point location.

■ **Solution**

From Eq. (7.30),

$$h_n = h_{\text{ac}_{\text{wb}}} + V_H \frac{a_t}{a}\left(1 - \frac{\partial \varepsilon}{\partial \alpha}\right)$$

where $h_{\text{ac}_{\text{wb}}} = 0.24$ (from Example 7.3). Thus,

$$h_n = 0.24 + 0.34\left(\frac{0.1}{0.08}\right)(1 - 0.35)$$

$$\boxed{h_n = 0.516}$$

Note from Example 7.3 that $h = 0.35$. Compare this center-of-gravity location with the neutral point location of 0.516. The center of gravity is comfortably *forward* of the neutral point; this again confirms the results of Example 7.5 that the airplane is statically stable.

7.11 STATIC MARGIN

A corollary to the preceding discussion can be obtained as follows. Solve Eq. (7.30) for $h_{\text{ac}_{\text{wb}}}$.

$$h_{\text{ac}_{\text{wb}}} = h_n - V_H \frac{a_t}{a}\left(1 - \frac{\partial \varepsilon}{\partial \alpha}\right) \tag{7.31}$$

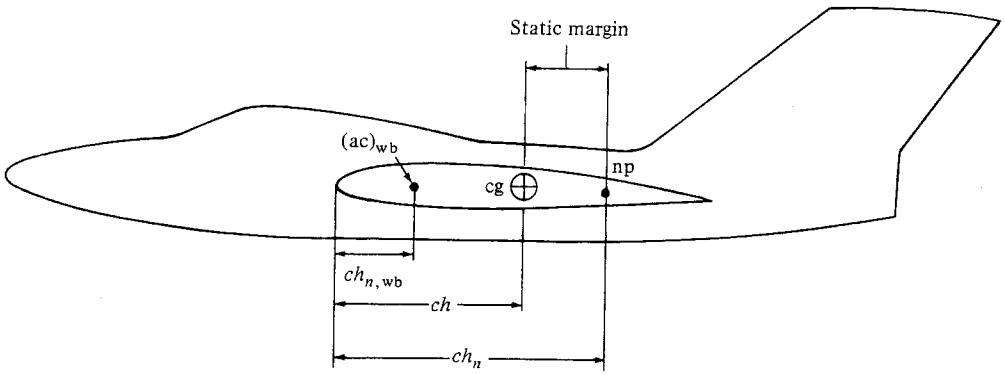

Figure 7.24 Illustration of the static margin.

Note that in Eqs. (7.29) to (7.31), the value of V_H is not precisely the same number as in Eq. (7.28). Indeed, in Eq. (7.28), V_H is based on the moment arm l_t measured from the center-of-gravity location, as shown in Fig. 7.21. In contrast, in Eq. (7.29), the center-of-gravity location has been moved to the neutral point, and V_H is therefore based on the moment arm measured from the neutral point location. However, the difference is usually small, and this effect will be ignored here. Therefore, substituting Eq. (7.31) into Eq. (7.28) and canceling the terms involving V_H, we obtain

$$\frac{\partial C_{M,\text{cg}}}{\partial \alpha_a} = a(h - h_n) \tag{7.32}$$

The distance $h_n - h$ is defined as the *static margin* and is illustrated in Fig. 7.24. Thus, from Eq. (7.32),

$$\frac{\partial C_{M,\text{cg}}}{\partial \alpha_a} = -a(h_n - h) = -a \times \text{static margin} \tag{7.33}$$

Equation (7.33) shows that the static margin is a direct measure of longitudinal static stability. For static stability, the static margin must be positive. Moreover, the larger the static margin, the more stable the airplane.

EXAMPLE 7.7

For the wind tunnel model of the previous examples, calculate the static margin.

■ **Solution**

From Example 7.6, $h_n = 0.516$ and $h = 0.35$. Thus, by definition,

$$\text{Static margin} \equiv h_n - h = 0.516 - 0.35 = \boxed{0.166}$$

For a check on the consistency of our calculations, consider Eq. (7.33).

$$\frac{\partial C_{M,\text{cg}}}{\partial \alpha_0} = -a \times \text{static margin} = -0.08(0.166) = -0.0133 \text{ per degree}$$

This is the same value calculated in Example 7.5; our calculations are indeed consistent.

DESIGN BOX

Let us boil down all the previous discussion to some plain speaking about the location of the lift force acting on the airplane relative to the center of gravity when the airplane is statically stable and when it is trimmed. Such plain speaking helps the airplane designer to have a clearer concept of how to design for a specified amount of stability (or instability).

A diagram that is frequently shown for a *statically stable* airplane is sketched in Fig. 7.25*a*. Here we will see the lift acting through a point situated *behind* the center of gravity, and we say this is necessary for static stability. But what does this really mean? What is the real significance of Fig. 7.25*a*? Let us look at it more closely.

First, recall that the lift of the airplane is due to the component of the net integrated pressure distribution exerted over the external surface of the airplane—the wings, fuselage, tail, etc.—acting perpendicular to the relative wind. This pressure distribution exerts a *distributed* load over the whole airplane. However, as is frequently done, we can conceptualize the mechanical effect of this distributed load by replacing it with a single concentrated force acting through an arbitrary point plus the moments acting about the same point. This is what is shown in Fig. 7.25*a*; we show the lift as a single concentrated force acting through a point, and we also indicate the moments about this point. The point that is chosen in Fig. 7.25*a* is the aerodynamic center of the airplane (the neutral point). In Fig. 7.25*a*, the lift shown is the *total* lift of the airplane, including the contribution from the tail.

In Sec. 7.10 we demonstrated that the aerodynamic center (neutral point) must be located behind the center of gravity in order to have static stability. We now have a simple picture in Fig. 7.25*b* that easily proves this. In Fig. 7.25*a* the airplane is trimmed; that is, $M_{cg} = 0$. Imagine that the airplane encounters a gust such that its angle of attack is momentarily increased. In turn, the lift will momentarily increase, as shown in Fig. 7.25*b*. Here, L_1 is the lift before the gust, and L_2 is the increased lift in response to the gust. Since the lift is acting through a point *behind* the center of gravity, the increased lift results in a

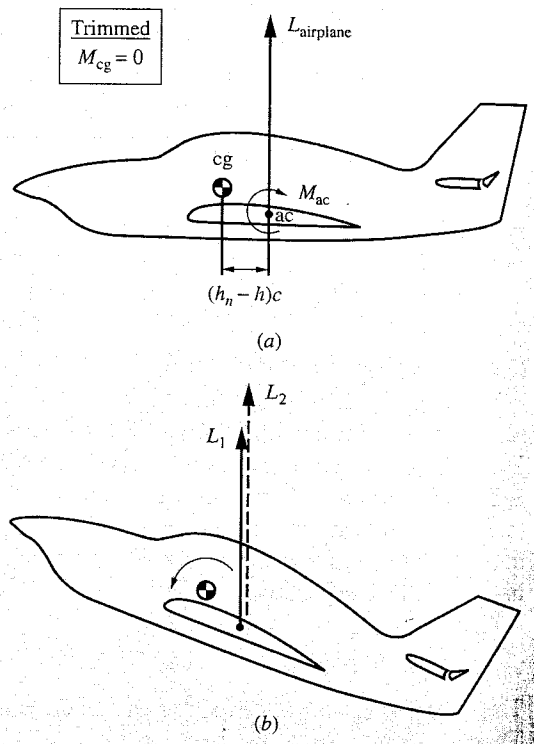

Figure 7.25 A diagram for static stability, with the lift acting behind the center of gravity.

negative (pitch-down) moment about the center of gravity, as shown in Fig. 7.25*b*. Hence, the initial tendency after encountering the gust will be to pitch the nose down, reducing the angle of attack and restoring the airplane to its trimmed condition—the precise notion of static stability. It is clear from Fig. 7.25 that if the lift acting through the aerodynamic center is *behind* the center of gravity, the airplane will be statically stable.

We note in passing that for the airplane in Fig. 7.25*a* to be trimmed, $M_{cg} = 0$. The lift is shown acting through the moment arm $(h_n - h)c$, hence creating a pitch-down moment about the center of gravity equal to $-[(h_n - h)cL]$. In turn, the moment about the aerodynamic center of the airplane M_{ac}

must be equal and opposite in order to have zero total moments about the center of gravity. That is, M_{ac} must be a positive (pitch-up) moment, as shown in Fig. 7.25*a*. Usually, much of this pitch-up moment is due to a download on the tail, similar to that illustrated in Fig. 7.17*a*. If the airplane configuration were a canard, then the positive M_{ac} would be due to an upload on the canard, similar to that illustrated in Fig. 7.17*b*. Indeed, when the airplane designer is trying to make a choice between the conventional rear-tail and the canard configurations, this situation is one of the advantages listed in favor of the canard. In Fig. 7.25, the lift shown is the *total* lift of the airplane, equal to the weight in steady, level flight. For a conventional rear-tail configuration, the download on the tail requires the wing to produce more lift in order for the total lift to equal the weight. In contrast, with the canard configuration, the upload on the canard contributes to the overall lift, hence requiring less lift from the wing. In turn, this reduces the induced drag generated from the wing.

Figure 7.25 reflects a commonly shown diagram illustrating longitudinal static stability, with the lift shown acting behind the center of gravity. An alternative picture illustrating static stability is shown in Fig. 7.26. This picture is not so commonly seen, but it is perhaps a "purer" explanation of the nature of longitudinal static stability. Recall that the lift of the airplane is due to the net integrated effect of the pressure distribution acting over the entire surface of the airplane. This pressure distribution has a *centroid* (analogous to the centroid of an area or a solid, which you calculate from differential calculus). The centroid of the pressure distribution is called the *center of pressure*. The center of pressure, being a centroid, is that point about which the net moment due to the distributed pressure is zero. Hence, when we simulate the mechanical effect of the distributed pressure distribution by a single concentrated force, it is most natural to locate this concentrated force at the center of pressure. Indeed, the center of pressure can be thought of as "that point on the airplane through which the lift effectively acts." To be more specific, we can simulate the mechanical effect of the distributed pressure loads on the airplane by first locating the center of pressure and then drawing the lift through this point, with zero moments about this point. This is the diagram shown in Fig. 7.26. Moreover, *when the airplane is trimmed, the center of pressure is precisely located at the center of gravity.*

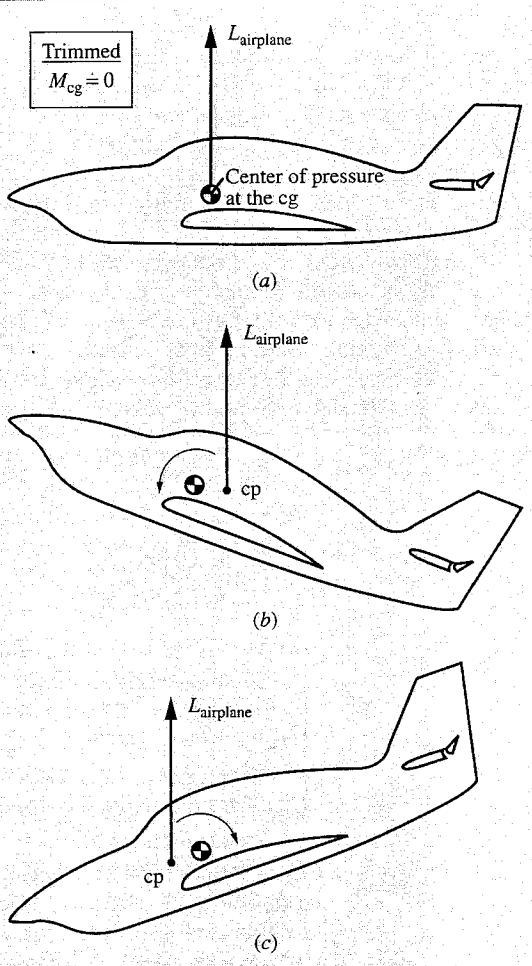

Figure 7.26 A diagram for static stability, with the lift acting at the center of pressure.

(continued on next page)

(continued from page 547)

This is the case shown in Fig. 7.26*a*; with the lift acting through the center of pressure and with the center of pressure at the center of gravity, there is no moment about the center of gravity, and by definition, the airplane is trimmed. This is what nature does. When the airplane is trimmed, the pressure distribution over the airplane has been adjusted so that the center of pressure is precisely at the center of gravity.

When the angle of attack of the airplane changes, the pressure distribution over the surface changes, and hence the center of pressure *shifts*—its location is a function of the angle of attack. For longitudinal static stability, the shift in the center of pressure must be in the direction shown in Fig. 7.26*b*. For static stability, the shift in the center of pressure must be *rearward*, to create a restoring moment about the center of gravity, as shown in Fig. 7.26*b*. Similarly, consider the originally trimmed airplane encountering a gust which *decreases* the angle of attack, as shown in Fig. 7.26*c*. For static stability, the shift in the center of pressure must be *forward* in order to create a restoring moment about the center of gravity, as shown in Fig. 7.26*c*. Hence, a statically stable airplane must be designed to have the shifts of the center of pressure in the directions shown in Fig. 7.26*b* and *c*.

In summary, Figs. 7.25 and 7.26 are alternative but equally effective diagrams to illustrate the necessary condition for longitudinal static stability. These figures supplement, and are totally consistent with, the more detailed mathematical descriptions in Secs. 7.6 to 7.11.

7.12 CONCEPT OF STATIC LONGITUDINAL CONTROL

A study of stability and control is double-barreled. The first aspect—that of stability itself—has been the subject of the preceding sections. However, for the remainder of this chapter, the focus will turn to the second aspect—control. In regard to our road map in Fig. 7.5, we are moving to the right-hand column.

Consider a statically stable airplane in trimmed (equilibrium) flight. Recalling Fig. 7.13, we see that the airplane must therefore be flying at the trim angle of attack α_e. In turn, this value of α_e corresponds to a definite value of lift coefficient, namely, the trim lift coefficient $C_{L_{\text{trim}}}$. For steady, level flight, this corresponds to a definite velocity, which from Eq. (6.26) is

$$V_{\text{trim}} = \sqrt{\frac{2W}{\rho_\infty S C_{L_{\text{trim}}}}} \tag{7.34}$$

Now assume that the pilot wishes to fly at a lower velocity $V_\infty < V_{\text{trim}}$. At a lower velocity, the lift coefficient, hence the angle of attack, must be increased to offset the decrease in dynamic pressure (remember from Chap. 6 that the lift must always balance the weight for steady, level flight). However, from Fig. 7.13, if α is increased, $C_{M,\text{cg}}$ becomes negative (i.e., the moment about the center of gravity is no longer zero), and the airplane is no longer trimmed. Consequently, if nothing else is changed about the airplane, it cannot achieve steady, level, equilibrium flight at any other velocity than V_{trim} or at any other angle of attack than α_e.

Obviously, this is an intolerable situation—an airplane must be able to change its velocity at the will of the pilot and still remain balanced. The only way

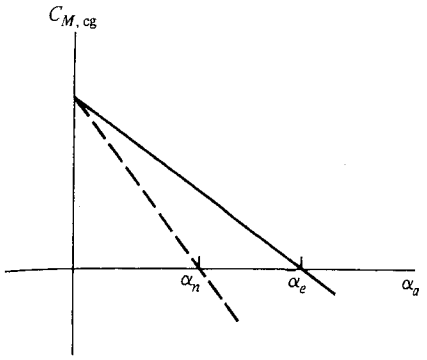

Figure 7.27 Change in trim angle of attack due to change in slope of moment coefficient curve.

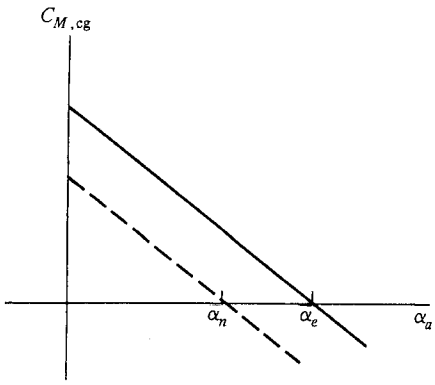

Figure 7.28 Change in trim angle of attack due to change in $C_{M,0}$.

to accomplish this is to effectively change the moment coefficient curve for the airplane. Say that the pilot wishes to fly at a *faster* velocity but still remain in steady, level, balanced flight. The lift coefficient must decrease, hence a new angle of attack α_n must be obtained, where $\alpha_n < \alpha_e$. At the same time, the moment coefficient curve must be changed such that $C_{M,cg} = 0$ at α_n. Figures 7.27 and 7.28 demonstrate two methods of achieving this change. In Fig. 7.27, the slope is made more negative, such that $C_{M,cg}$ goes through zero at α_n. From Eq. (7.28) or (7.32), the slope can be changed by shifting the center of gravity. In our example, the center of gravity must be shifted forward. Otto Lilienthal (see Sec. 1.5) used this method in his gliding flights. Figure 1.15 shows Lilienthal hanging loosely below his glider; by simply swinging his hips, he was able to shift the center of gravity and change the stability of the aircraft. This principle is carried over today to the modern hang gliders for sports use.

However, for a conventional airplane, shifting the center of gravity is highly impractical. Therefore, another method for changing the moment curve is employed, as shown in Fig. 7.28. Here, the slope remains the same, but $C_{M,0}$ is changed such that $C_{M,cg} = 0$ at α_n. This is accomplished by deflecting the elevator on the horizontal tail. Hence, we have arrived at a major concept of static, longitudinal control, namely, that the elevator deflection can be used to control the trim angle of attack, hence to control the equilibrium velocity of the airplane.

Consider Fig. 7.28. We stated earlier, without proof, that a translation of the moment curve without a change in slope can be obtained simply by deflecting the elevator. But *how* and *to what extent* does the elevator deflection change $C_{M,cg}$? To provide some answers, first consider the horizontal tail with the elevator fixed in the neutral position, that is, no elevator deflection, as shown in Fig. 7.29. The absolute angle of attack of the tail is α_t, as defined earlier. The variation of tail lift coefficient with α_t is also sketched in Fig. 7.29; note that it has the same general shape as the airfoil and wing lift curves discussed in Chap. 5. Now assume that the elevator is deflected downward through angle δ_e, as shown in Fig. 7.30. This is the

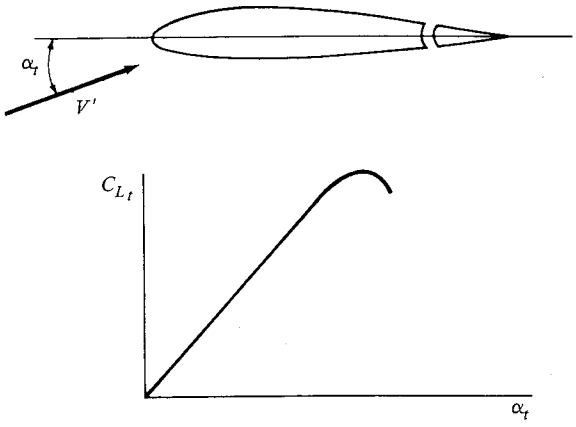

Figure 7.29 Tail lift coefficient curve with no elevator deflection.

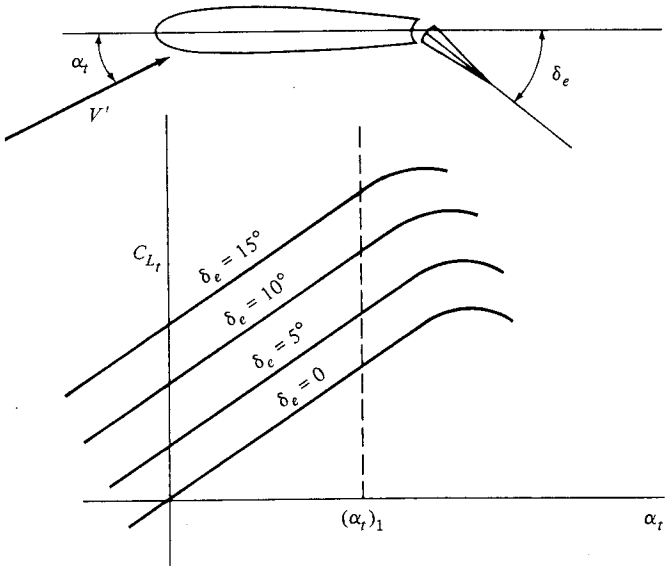

Figure 7.30 Tail lift coefficient with elevator deflection.

same picture as a wing with a deflected flap, as discussed in Sec. 5.17. Consequently, just as in the case of a deflected flap, the deflected elevator causes the tail lift coefficient curve to shift to the left, as shown in Fig. 7.30. By convention (and for convenience later), a downward elevator deflection is positive. Therefore, if the elevator is deflected by an angle of, say, 5° and then held fixed as the complete tail is pitched through a range of α_t, then the tail lift curve is translated to the left. If the elevator is then deflected farther, say to 10°, the lift curve is shifted even

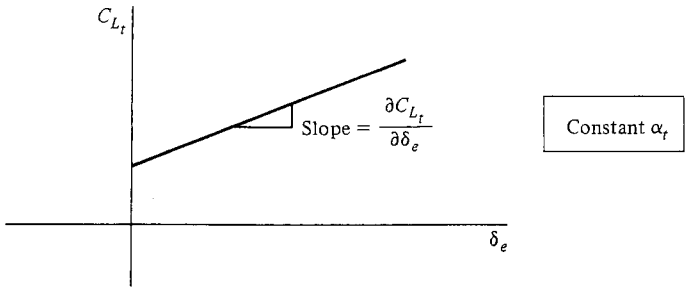

Figure 7.31 Tail lift coefficient versus elevator deflection at constant angle of attack; a cross-plot of Fig. 7.30.

farther to the left. This behavior is clearly illustrated in Fig. 7.30. Note that for all the lift curves, the slope $\partial C_{L,t}/\partial \alpha_t$ is the same.

With the preceding discussion in mind, now consider the tail at a fixed angle of attack, say, $(\alpha_t)_1$. If the elevator is deflected from, say, 0 to 15°, then $C_{L,t}$ will increase along the vertical dashed line in Fig. 7.30. This variation can be cross-plotted as $C_{L,t}$ versus δ_e, as shown in Fig. 7.31. For most conventional airplanes, the curve in Fig. 7.31 is essentially linear, and its slope $\partial C_{L,t}/\partial \delta_e$ is called the *elevator control effectiveness*. This quantity is a direct measure of the "strength" of the elevator as a control; because δ_e has been defined as positive for downward deflections, $\partial C_{L,t}/\partial \delta_e$ is *always positive*.

Consequently, the tail lift coefficient is a function of *both* α_t and δ_e (hence, the partial derivative notation is used, as discussed earlier). Keep in mind that, physically, $\partial C_{L,t}/\partial \alpha_t$ is the rate of change of $C_{L,t}$ with respect to α_t, keeping δ_e constant; similarly, $\partial C_{L,t}/\partial \delta_e$ is the rate of change of $C_{L,t}$ with respect to δ_e, keeping α_t constant. Hence, on a physical basis,

$$C_{L,t} = \frac{\partial C_{L,t}}{\partial \alpha_t}\alpha_t + \frac{\partial C_{L,t}}{\partial \delta_e}\delta_e \tag{7.35}$$

Recalling that the tail lift slope is $a_t = \partial C_{L,t}/\partial \alpha_t$, we see that Eq. (7.35) can be written as

$$C_{L,t} = a_t \alpha_t + \frac{\partial C_{L,t}}{\partial \delta_e}\delta_e \tag{7.36}$$

Substituting Eq. (7.36) into (7.24), we have for the pitching moment about the center of gravity

$$\boxed{C_{M,\mathrm{cg}} = C_{M,\mathrm{ac_{wb}}} + C_{L,\mathrm{wb}}(h - h_{\mathrm{ac}}) - V_H\left(a_t\alpha_t + \frac{\partial C_{L,t}}{\partial \delta_e}\delta_e\right)} \tag{7.37}$$

Equation (7.37) gives explicitly the effect of elevator deflection on moments about the center of gravity of the airplane.

The rate of change of $C_{M,\mathrm{cg}}$ due *only* to elevator deflection is, by definition, $\partial C_{M,\mathrm{cg}}/\partial \delta_e$. This partial derivative can be found by differentiating Eq. (7.37)

with respect to δ_e, keeping everything else constant.

$$\frac{\partial C_{M,\text{cg}}}{\partial \delta_e} = -V_H \frac{\partial C_{L,t}}{\partial \delta_e} \tag{7.38}$$

Note that, from Fig. 7.31, $\partial C_{L,t}/\partial \delta_e$ is constant; moreover, V_H is a specific value for the given airplane. Thus, the right-hand side of Eq. (7.38) is a constant. Therefore, on a physical basis, the increment in $C_{M,\text{cg}}$ due *only* to a given elevator deflection δ_e is

$$\Delta C_{M,\text{cg}} = -V_H \frac{\partial C_{L,t}}{\partial \delta_e} \delta_e \tag{7.39}$$

Equation (7.39) now answers the questions asked earlier concerning how and to what extent the elevator deflection changes $C_{M,\text{cg}}$. Consider the moment curve labeled $\delta_e = 0$ in Fig. 7.32. This is the curve with the elevator fixed in the neutral position; it is the curve we originally introduced in Fig. 7.13. If the elevator is now deflected through a positive angle (downward), Eq. (7.39) states that all points on this curve will be shifted down by the constant amount $\Delta C_{M,\text{cg}}$. Hence, the slope of the moment curve is preserved; only the value of $C_{M,0}$ is changed by elevator deflection. This now proves our earlier statement made in conjunction with Fig. 7.28.

For emphasis, we repeat the main thrust of this section. The elevator can be used to change and control the trim of the airplane. In essence, this controls the equilibrium velocity of the airplane. For example, by a downward deflection of the elevator, a new trim angle α_n smaller than the original trim angle α_e can be obtained. (This is illustrated in Fig. 7.32.) This corresponds to an increase in velocity of the airplane.

As another example, consider the two velocity extremes—stalling velocity and maximum velocity. Figure 7.33 illustrates the elevator deflection necessary to

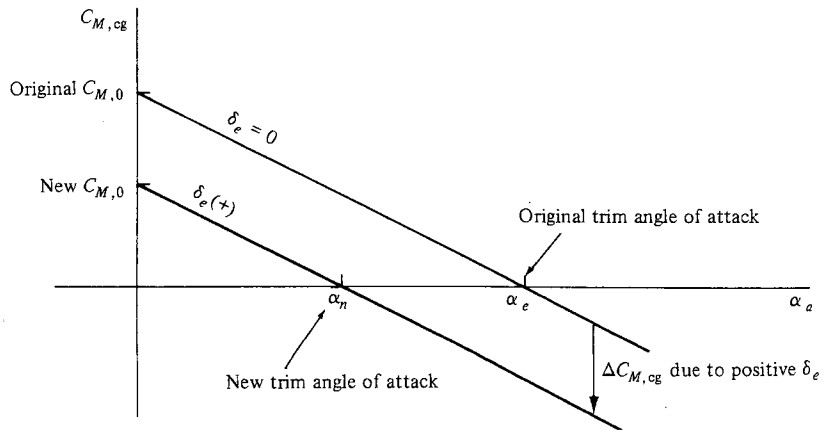

Figure 7.32 Effect of elevator deflection on moment coefficient.

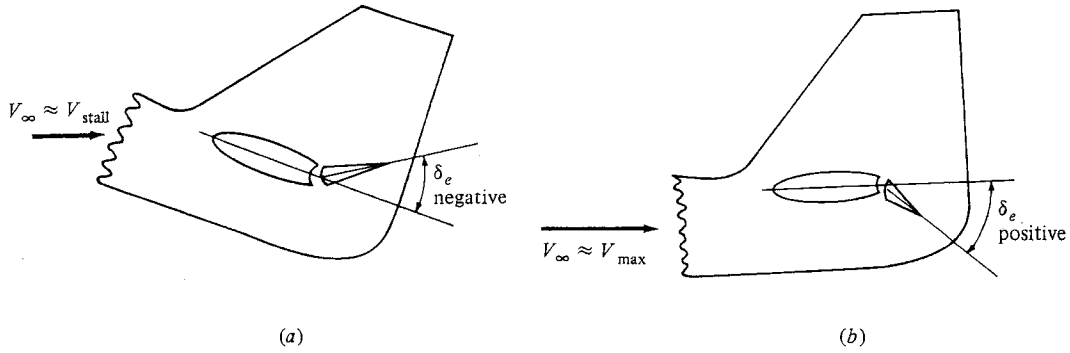

Figure 7.33 Elevator deflection required for trim at (*a*) low flight velocity and (*b*) high flight velocity.

trim the airplane at these two extremes. First consider Fig. 7.33*a*, which corresponds to an airplane flying at $V_\infty \approx V_{stall}$. This would be the situation on a landing approach, for example. The airplane is flying at $C_{L_{max}}$; hence, the angle of attack is large. Therefore, from our previous discussion, the airplane must be trimmed by an *up-elevator* position, that is, by a negative δ_e. On the other hand, consider Fig. 7.33*b*, which corresponds to an airplane flying at $V_\infty \approx V_{max}$ (near full throttle). Because q_∞ is large, the airplane requires only a small C_L to generate the required lift force; hence, the angle of attack is small. Thus, the airplane must be trimmed by a *down-elevator* position, that is, by a positive δ_e.

7.13 CALCULATION OF ELEVATOR ANGLE TO TRIM

The concepts and relations developed in Sec. 7.12 allow us now to calculate the precise elevator deflection necessary to trim the airplane at a given angle of attack. Consider an airplane with its moment coefficient curve given as in Fig. 7.34. The equilibrium angle of attack with no elevator deflection is α_e. We wish to trim the airplane at a new angle of attack α_n. What value of δ_e is required for this purpose?

To answer this question, first write the equation for the moment curve with $\delta_e = 0$ (the solid line in Fig. 7.34). This is a straight line with a constant slope equal to $\partial C_{M,cg}/\partial \alpha_a$ and intercepting the ordinate at $C_{M,0}$. Hence, from analytic geometry, the equation of this line is

$$C_{M,cg} = C_{M,0} + \frac{\partial C_{M,cg}}{\partial \alpha_a} \alpha_a \tag{7.40}$$

Now assume the elevator is deflected through an angle δ_e. The value of $C_{M,cg}$ will change by the increment $\Delta C_{M,cg}$, and the moment equation given by Eq. (7.40) is now modified as

$$C_{M,cg} = C_{M,0} + \frac{\partial C_{M,cg}}{\partial \alpha_a} \alpha_a + \Delta C_{M,cg} \tag{7.41}$$

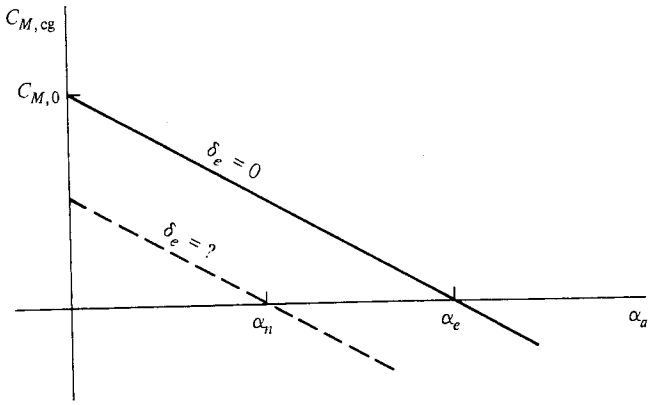

Figure 7.34 Given the equilibrium angle of attack at zero elevator deflection, what elevator deflection is necessary to establish a given new equilibrium angle of attack?

The value of $\Delta C_{M,cg}$ was obtained earlier as Eq. (7.39). Hence, substituting Eq. (7.39) into (7.41), we obtain

$$C_{M,cg} = C_{M,0} + \frac{\partial C_{M,cg}}{\partial \alpha_a} \alpha_a - V_H \frac{\partial C_{L,t}}{\partial \delta_e} \delta_e \tag{7.42}$$

Equation (7.42) allows us to calculate $C_{M,cg}$ for any arbitrary angle of attack α_a and any arbitrary elevator deflection δ_e. However, we are interested in the specific situation where $C_{M,cg} = 0$ at $\alpha_a = \alpha_n$ and where the value of δ_e necessary to obtain this condition is $\delta_e = \delta_{trim}$. That is, we want to find the value of δ_e, which gives the dashed line in Fig. 7.34. Substituting the preceding values into Eq. (7.42), we have

$$0 = C_{M,0} + \frac{\partial C_{M,cg}}{\partial \alpha_a} \alpha_n - V_H \frac{\partial C_{L,t}}{\partial \delta_e} \delta_{trim}$$

and solving for δ_{trim}, we obtain

$$\boxed{\delta_{trim} = \frac{C_{M,0} + (\partial C_{M,cg}/\partial \alpha_a)\alpha_n}{V_H(\partial C_{L,t}/\partial \delta_e)}} \tag{7.43}$$

Equation (7.43) is the desired result. It gives the elevator deflection necessary to trim the airplane at a given angle of attack α_n. In Eq. (7.43), V_H is a known value from the airplane design, and $C_{M,0}$, $\partial C_{M,cg}/\partial \alpha_a$, and $\partial C_{L,t}/\partial \delta_e$ are known values usually obtained from wind tunnel or free-flight data.

EXAMPLE 7.8

Consider a full-size airplane with the same aerodynamic and design characteristics as the wind tunnel model of Examples 7.3 to 7.7. The airplane has a wing area of 19 m^2, a weight of 2.27×10^4 N, and an elevator control effectiveness of 0.04. Calculate the elevator deflection angle necessary to trim the airplane at a velocity of 61 m/s at sea level.

Solution

First, we must calculate the angle of attack for the airplane at $V_\infty = 61$ m/s. Recall that

$$C_L = \frac{2W}{\rho_\infty V_\infty^2 S} = \frac{2(2.27 \times 10^4)}{1.225(61)^2(19)} = 0.52$$

From Example 7.3, the lift slope is $a = 0.08$ per degree. Hence, the absolute angle of attack of the airplane is

$$\alpha_a = \frac{C_L}{a} = \frac{0.52}{0.08} = 6.5°$$

From Eq. (7.43), the elevator deflection angle required to trim the airplane at this angle of attack is

$$\delta_{\text{trim}} = \frac{C_{M,0} + (\partial C_{M,\text{cg}}/\partial \alpha_a)\alpha_n}{V_H(\partial C_{L,t}/\partial \delta_e)}$$

where

$C_{M,0} = 0.06$	(from Example 7.5)
$\frac{C_{M,\text{cg}}}{\partial \alpha_a} = -0.0133$	(from Example 7.5)
$\alpha_n = 6.5°$	(this is the α_a calculated previously)
$V_H = 0.34$	(from Example 7.4)
$\frac{\partial C_{L,t}}{\partial \delta_e} = 0.04$	(given in the preceding information)

Thus, from Eq. (7.43),

$$\delta_{\text{trim}} = \frac{0.06 + (-0.0133)(6.5)}{0.34(0.04)} = \boxed{-1.94°}$$

Recall that positive δ is downward. Hence, to trim the airplane at an angle of attack of 6.5°, the elevator must be deflected *upward* by 1.94°.

7.14 STICK-FIXED VERSUS STICK-FREE STATIC STABILITY

The second paragraph of Sec. 7.5 initiated our study of a rigid airplane with *fixed controls,* for example, the elevator *fixed* at a given deflection angle. The ensuing sections developed the static stability for such a case, always assuming that the elevator can be deflected to a desired angle δ_e but held fixed at that angle. This is the situation when the pilot (human or automatic) moves the control stick to a given position and then rigidly holds it there. Consequently, the static stability that we have discussed to this point is called *stick-fixed static stability.* Modern high-performance airplanes designed to fly near or beyond the speed of sound have hydraulically assisted power controls; therefore, a stick-fixed static stability analysis is appropriate for such airplanes.

However, consider a control stick connected to the elevator via wire cables without a power boost of any sort. This was characteristic of most early airplanes until the 1940s and is representative of many light, general aviation, private aircraft of today. In this case, to hold the stick fixed in a given position, the pilot must continually exert a manual force. This is uncomfortable and impractical. Consequently, in steady, level flight, the control stick is left essentially free; in turn, the elevator is left free to float under the influence of the natural aerodynamic forces and moments at the tail. The static stability of such an airplane is therefore called *stick-free static stability*. This is the subject of Secs. 7.15 and 7.16.

7.15 ELEVATOR HINGE MOMENT

Consider a horizontal tail with an elevator that rotates about a hinge axis, as shown in Fig. 7.35. Assume the airfoil section of the tail is symmetric, which is almost always the case for both the horizontal and vertical tail. First, consider the tail at zero angle of attack, as shown in Fig. 7.35*a*. The aerodynamic pressure distribution on the top and bottom surfaces of the elevator will be the same, that is, symmetric about the chord. Hence, there will be no moment exerted on the elevator about the hinge line. Now assume that the tail is pitched to the angle of attack α_t, but the elevator is not deflected; that is, $\delta_e = 0$. This is illustrated in Fig. 7.35*b*. As discussed in Chap. 5, there will be a low pressure on the top surface of the airfoil and a high pressure on the bottom surface. Consequently, the aerodynamic force on the elevator will not be balanced, and there will be a moment about the hinge axis tending to deflect the elevator upward. Finally, consider the horizontal tail at zero angle of attack but with the elevator deflected downward and held fixed at the angle δ_e, as shown in Fig. 7.35*c*. Recall from Sec. 5.17 that a flap deflection effectively changes the camber of the airfoil and alters the pressure distribution. Therefore, in Fig. 7.35*c*, there will be low and high pressures on the top and bottom elevator surfaces, respectively. As a result, a moment will again be exerted about the hinge line, tending to rotate the elevator upward. Thus, we see that both the tail angle of attack α_t and the elevator deflection δ_e result in a moment about the elevator hinge line—such a moment is defined as the *elevator hinge moment*. It is the governing factor in stick-free static stability, as discussed in Sec. 7.16.

Let H_e denote the elevator hinge moment. Also, referring to Fig. 7.36, we see the chord of the tail is c_t, the distance from the leading edge of the elevator to the hinge line is c_b, the distance from the hinge line to the trailing edge is c_e, and that portion of the elevator planform area that lies *behind* (aft of) the hinge line is S_e. The *elevator hinge moment* coefficient C_{h_e} is then defined as

$$C_{h_e} = \frac{H_e}{\frac{1}{2}\rho_\infty V_\infty^2 S_e c_e} \tag{7.44}$$

where V_∞ is the free-stream velocity of the airplane.

Recall that the elevator hinge moment is due to the tail angle of attack and the elevator deflection. Hence, C_{h_e} is a function of both α_t and δ_e. Moreover,

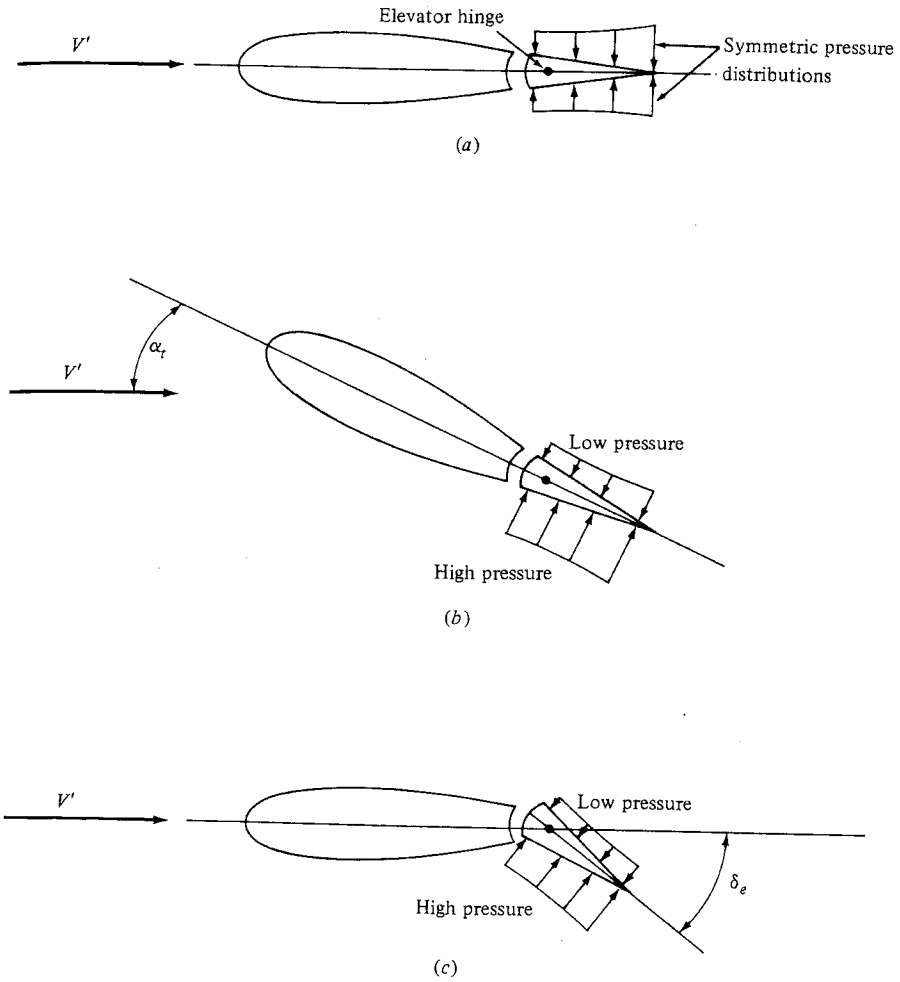

Figure 7.35 Illustration of the aerodynamic generation of elevator hinge moment. (*a*) No hinge moment; (*b*) hinge moment due to angle of attack; (*c*) hinge moment due to elevator deflection.

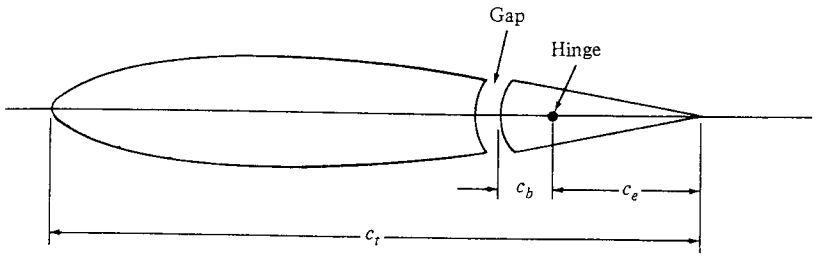

Figure 7.36 Nomenclature and geometry for hinge moment coefficient.

experience has shown that at both subsonic and supersonic speeds, C_{h_e} is approximately a linear function of α_t and δ_e. Thus, recalling the definition of the partial derivative in Sec. 7.2.4, we can write the hinge moment coefficient as

$$C_{h_e} = \frac{\partial C_{h_e}}{\partial \alpha_t} \alpha_t + \frac{\partial C_{h_e}}{\partial \delta_e} \delta_e \tag{7.45}$$

where $\partial C_{h_e}/\partial \alpha_t$ and $\partial C_{h_e}/\partial \delta_e$ are approximately constant. However, the actual magnitudes of these constant values depend in a complicated way on c_e/c_t, c_b/c_e, the elevator nose shape, gap, trailing-edge angle, and planform. Moreover, H_e is very sensitive to local boundary layer separation. As a result, the values of the partial derivatives in Eq. (7.45) must almost always be obtained empirically, such as from wind tunnel tests, for a given design.

Consistent with the convention that downward elevator deflections are positive, hinge moments that tend to deflect the elevator downward are also defined as positive. Note from Fig. 7.35*b* that a positive α_t physically tends to produce a negative hinge moment (tending to deflect the elevator upward). Hence, $\partial C_{h_e}/\partial \alpha_t$ is usually negative. (However, if the hinge axis is placed very far back, near the trailing edge, the sense of H_e may become positive. This is usually not done for conventional airplanes.) Also, note from Fig. 7.35*c* that a positive δ_e usually produces a negative H_e; hence, $\partial C_{h_e}/\partial \delta_e$ is also negative.

7.16 STICK-FREE LONGITUDINAL STATIC STABILITY

Let us return to the concept of stick-free static stability introduced in Sec. 7.14. If the elevator is left free to float, it will always seek some equilibrium deflection angle such that the hinge moment is zero; that is, $H_e = 0$. This is obvious, because as long as there is a moment on the free elevator, it will always rotate. It will come to rest (equilibrium) only for that position where the moment is zero.

Recall our qualitative discussion of longitudinal static stability in Sec. 7.5. Imagine that an airplane is flying in steady, level flight at the equilibrium angle of attack. Now assume the airplane is disturbed by a wind gust and is momentarily pitched to another angle of attack, as sketched in Fig. 7.14. If the airplane is statically stable, it will initially tend to return toward its equilibrium position. In subsequent sections, we saw that the design of the horizontal tail was a powerful mechanism governing this static stability. However, until now, the elevator was always considered fixed. But if the elevator is allowed to float freely when the airplane is pitched by some disturbance, the elevator will seek some momentary equilibrium position different from its position before the disturbance. This deflection of the free elevator will change the static stability characteristics of the airplane. In fact, such stick-free stability is usually less than stick-fixed stability. For this reason, it is usually desirable to design an airplane such that the difference between stick-free and stick-fixed longitudinal stability is small.

With this in mind, consider the equilibrium deflection angle of a free elevator. Denote this angle by δ_{free}, as sketched in Fig. 7.37. At this angle, $H_e = 0$.

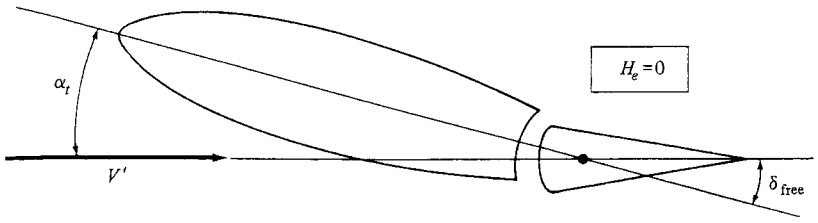

Figure 7.37 Illustration of free elevator deflection.

Thus, from Eq. (7.45),

$$C_{h_e} = 0 = \frac{\partial C_{h_e}}{\partial \alpha_t} \alpha_t + \frac{\partial C_{h_e}}{\partial \delta_e} \delta_{\text{free}} \tag{7.46}$$

Solving Eq. (7.46) for δ_{free} gives

$$\boxed{\delta_{\text{free}} = -\frac{\partial C_{h_e}/\partial \alpha_t}{\partial C_{h_e}/\partial \delta_e} \alpha_t} \tag{7.47}$$

Equation (7.47) gives the equilibrium, free-floating angle of the elevator as a function of tail angle of attack. As stated earlier, both partial derivatives in Eq. (7.47) are usually negative; hence, a positive α_t yields a negative δ_{free} (an upward deflection). This is intuitively correct, as verified by Fig. 7.37, which shows a negative δ_{free}.

Obviously, δ_{free} affects the tail lift coefficient, which, in turn, affects the static stability of the airplane. The tail lift coefficient for angle of attack α_t and fixed-elevator deflection δ_e was given in Eq. (7.36), repeated here:

$$C_{L,t} = a_t \alpha_t + \frac{\partial C_{L,t}}{\partial \delta_e} \delta_e$$

However, for a free elevator, $\delta_e = \delta_{\text{free}}$. Denoting the tail lift coefficient for a free elevator as $C'_{L,t}$, we see that a substitution of Eq. (7.47) into (7.36) gives

$$C'_{L,t} = a_t \alpha_t + \frac{\partial C_{L,t}}{\partial \delta_e} \delta_{\text{free}}$$

$$C'_{L,t} = a_t \alpha_t - \frac{\partial C_{L,t}}{\partial \delta_e} \frac{\partial C_{h_e}/\partial \alpha_t}{\partial C_{h_e}/\partial \delta_e} \alpha_t$$

or

$$\boxed{C'_{L,t} = a_t \alpha_t F} \tag{7.48}$$

where F is the *free elevator factor*, defined as

$$F = 1 - \frac{1}{a_t} \frac{\partial C_{L,t}}{\partial \delta_e} \frac{\partial C_{h_e}/\partial \alpha_t}{\partial C_{h_e}/\partial \delta_e}$$

The free elevator factor is a number usually less than unity and usually on the order of 0.7 to 0.8. It represents a reduction in the tail's contribution to static stability when the elevator is free. The magnitude of this reduction is developed in the following.

Consider now the moment about the center of gravity of the airplane. For a fixed elevator, the moment coefficient is given by Eq. (7.24),

$$C_{M,\text{cg}} = C_{M,\text{ac}_{\text{wb}}} + C_{L_{\text{wb}}}(h - h_{\text{ac}_{\text{wb}}}) - V_H C_{L,t}$$

For a free elevator, the tail lift coefficient is now changed to $C'_{L,t}$. Hence, the moment coefficient for a free elevator $C'_{M,\text{cg}}$ is

$$C'_{M,\text{cg}} = C_{M,\text{ac}_{\text{wb}}} + C_{L_{\text{wb}}}(h - h_{\text{ac}_{\text{wb}}}) - V_H C'_{L,t} \tag{7.49}$$

Substituting Eq. (7.48) into (7.49), we get

$$\boxed{C'_{M,\text{cg}} = C_{M,\text{ac}_{\text{wb}}} + C_{L_{\text{wb}}}(h - h_{\text{ac}_{\text{wb}}}) - V_H a_t \alpha_t F} \tag{7.50}$$

Equation (7.50) gives the final form of the moment coefficient about the center of gravity of the airplane with a free elevator.

By using Eq. (7.50), the same analyses as given in Sec. 7.9 can be used to obtain equations for stick-free longitudinal static stability. The results are as follows:

$$C'_{M,0} = C_{M,\text{ac}_{\text{wb}}} + F V_H a_t (i_t + \varepsilon_0) \tag{7.51}$$

$$h'_n = h_{\text{ac}_{\text{wb}}} + F V_H \frac{a_t}{a}\left(1 - \frac{\partial \varepsilon}{\partial \alpha}\right) \tag{7.52}$$

$$\frac{\partial C'_{M,\text{cg}}}{\partial \alpha} = -a(h'_n - h) \tag{7.53}$$

Equations (7.51), (7.52), and (7.53) apply for stick-free conditions, denoted by the prime notation. They should be compared with Eqs. (7.27), (7.30), and (7.33), respectively, for stick-fixed stability. Note that $h'_n - h$ is the stick-free static margin; because $F < 1.0$, this is smaller than the stick-fixed static margin.

Hence, it is clear from Eqs. (7.51) to (7.53) that a free elevator usually decreases the static stability of the airplane.

EXAMPLE 7.9

Consider the airplane of Example 7.8. Its elevator hinge moment derivatives are $\partial C_{h_e}/\partial \alpha_t = -0.008$ and $\partial C_{h_e}/\partial \delta_e = -0.013$. Assess the *stick-free* static stability of this airplane.

■ Solution

First, obtain the free elevator factor F, defined from Eq. (7.48),

$$F = 1 - \frac{1}{a_t}\frac{\partial C_{L,t}}{\partial \delta_e}\frac{\partial C_{h_e}/\partial \alpha_t}{\partial C_{h_e}/\partial \delta_e}$$

where $a_t = 0.1$ (from Example 7.4)

$$\frac{\partial C_{L,t}}{\partial \delta_e} = 0.04 \quad \text{(from Example 7.8)}$$

$$F = 1 - \frac{1}{0.1}(0.04)\left(\frac{-0.008}{-0.013}\right) = 0.754$$

The stick-free static stability characteristics are given by Eqs. (7.51) to (7.53). First, from Eq. (7.51),

$$C'_{M,0} = C_{M,\text{ac}_{wb}} + FV_H a_t (i_t + \varepsilon_0)$$

where $C_{M,\text{ac}_{wb}} = -0.032$ (from Example 7.3)
$V_H = 0.34$ (from Example 7.4)
$i_t = 2.7°$ (from Example 7.4)
$\varepsilon_0 = 0$ (from Example 7.4)

Thus, $$C'_{M,0} = -0.032 + 0.754(0.34)(0.1)(2.7)$$

$$\boxed{C'_{M,0} = 0.037}$$

This is to be compared with $C_{M,0} = 0.06$ obtained for stick-fixed conditions in Example 7.5.

From Eq. (7.52),

$$h'_n = h_{\text{ac}_{wb}} + FV_H \frac{a_t}{a}\left(1 - \frac{\partial \varepsilon}{\partial \alpha}\right)$$

where $h_{\text{ac}_{wb}} = 0.24$ (from Example 7.3)
$\frac{\partial \varepsilon}{\partial \alpha} = 0.35$ (from Example 7.4)
$a = 0.08$ (from Example 7.4)

$$h'_n = 0.24 + 0.754(0.34)\left(\frac{0.1}{0.08}\right)(1 - 0.35)$$

$$\boxed{h'_n = 0.448}$$

This is to be compared with $h_n = 0.516$ obtained for stick-fixed conditions in Example 7.6. Note that the neutral point has moved forward for stick-free conditions, hence decreasing the stability. In fact, the stick-free static margin is

$$h'_n - h = 0.448 - 0.35 = 0.098$$

This is a 41 percent decrease, in comparison with the stick-fixed static margin from Example 7.7. Finally, from Eq. (7.53),

$$\frac{\partial C'_{M,\text{cg}}}{\partial \alpha} = -a(h'_n - h) = -0.08(0.098) = \boxed{-0.0078}$$

Thus, as expected, the slope of the stick-free moment coefficient curve, although still negative, is small in absolute value.

In conclusion, this problem indicates that stick-free conditions cut the static stability of our hypothetical airplane by nearly one-half. This helps to dramatize the differences between stick-fixed and stick-free considerations.

7.17 DIRECTIONAL STATIC STABILITY

Returning to Fig. 7.2, we note that the preceding sections have dealt with longitudinal stability and control, which concerns angular motion about the y axis—pitching motion. In this section, we briefly examine the stability associated with angular motion about the z axis—yawing motion. Stability in yaw is called *directional stability*. In regard to our road map in Fig. 7.5, we are moving to the second box at the bottom of the left-hand column.

Examining Fig. 7.3, we see the vertical stabilizer (vertical fin, or vertical tail) is the conventional mechanism for directional stability. Its function is easily seen in Fig. 7.38. Consider an airplane in equilibrium flight with no yaw, as sketched in Fig. 7.38*a*. The vertical tail, which is designed with a symmetric airfoil section, is at zero angle of attack to the free stream, and it experiences no net aerodynamic force perpendicular to V_∞. Assume the airplane is suddenly yawed to the right by a disturbance, as shown in Fig. 7.38*b*. The vertical tail is now at an angle of attack θ and experiences an aerodynamic force F_{vt} perpendicular to V_∞. This force creates a restoring yawing moment about the center of gravity that tends to rotate the airplane back toward its equilibrium position. The same situation prevails when the airplane is yawed to the left by a disturbance, as sketched in Fig. 7.38*c*.

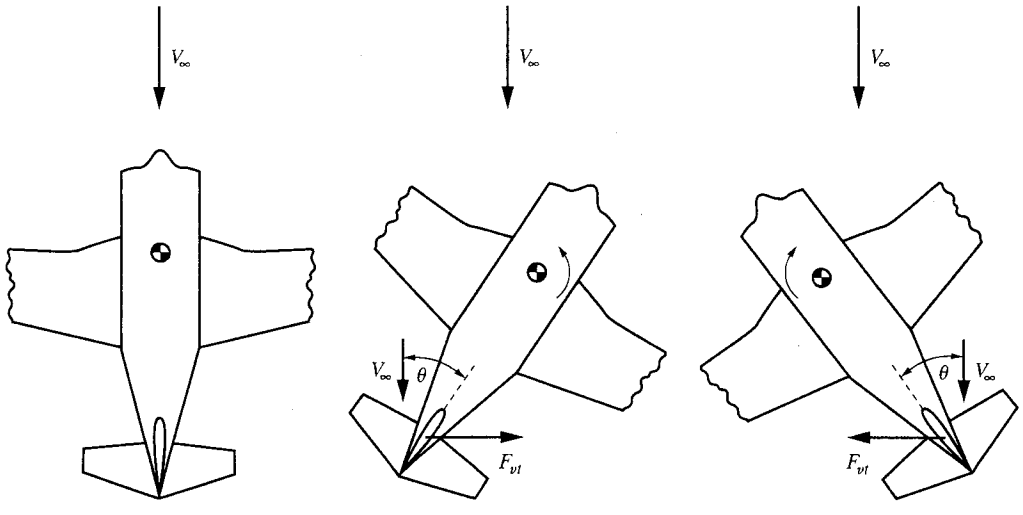

(*a*) No yaw (*b*) Yaw to the right (*c*) Yaw to the left

Figure 7.38 Effect of the vertical stabilizer on directional stability.

DESIGN BOX

For conventional airplanes, typical values of V_{vt} are given by Raymer (see Bibliography) as follows:

	V_{vt}
General aviation, single-engine	0.04
Twin turboprop	0.08
Jet fighter	0.07
Jet transport	0.09

These numbers are considerably smaller than typical values of V_H, which range from 0.4 to 1.0 (in Example 7.4, we used $V_H = 0.34$), because of the use of b rather than c in the definition of V_{vt}.

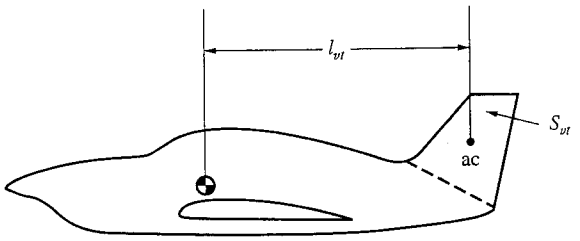

Figure 7.39 Moment arm of the vertical tail.

The magnitude of the restoring moment in yaw is equal to $F_{vt}l_{vt}$, where l_{vt} is the moment arm from the aerodynamic center of the vertical tail to the airplane's center of gravity, as shown in Fig. 7.39. Since the aerodynamic force on the vertical tail F_{vt} is proportional to the area of the vertical tail S_{vt}, shown as the shaded area in Fig. 7.39, the design parameter governing directional stability can be shown to be the vertical tail volume ratio, defined as

$$\text{Vertical tail volume ratio} \equiv V_{vt} \equiv \frac{l_{vt}S_{vt}}{bS} \tag{7.54}$$

where b is the wingspan and S is the wing planform area. The definition of V_{vt} in Eq. (7.54) is similar to the definition of the horizontal tail volume ratio V_H defined by Eq. (7.16), except that V_{vt} uses b rather than the chord c as the nondimensionalizing length in the denominator.

7.18 LATERAL STATIC STABILITY

Return to Fig. 7.2. In this section we briefly examine the stability associated with angular motion about the x axis—rolling motion. Stability in roll is called *lateral stability*. In regard to our road map in Fig. 7.5, we are moving to the third box at the bottom of the left-hand column.

Consider an airplane in steady, level flight. Let us take a view of this airplane from behind, looking in the direction of flight, as sketched in Fig. 7.40*a*. The lift equals the weight. They act equal and opposite to each other; there is no net side

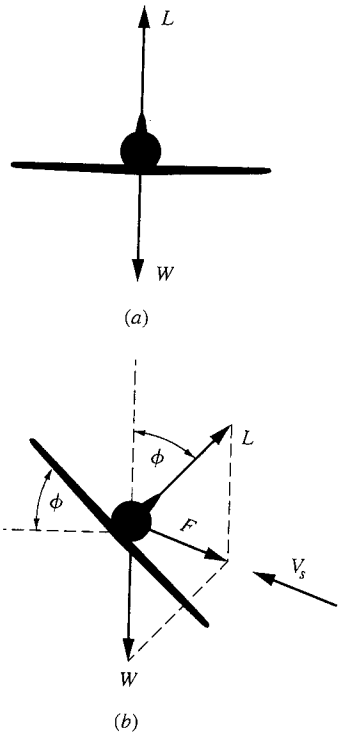

Figure 7.40 Generation of slideslip.

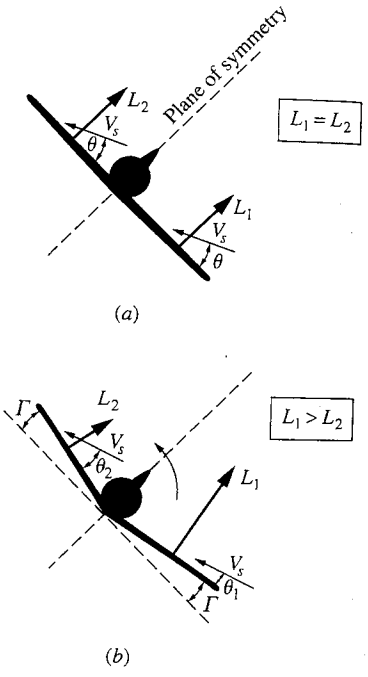

Figure 7.41 Effect of dihedral.

force. The airplane is suddenly perturbed by a gust that causes the right wing to dip; that is, a roll to the right ensues. This is sketched in Fig. 7.40*b*. The lift vector is now rotated from the vertical through angle ϕ, called the *bank angle*. The vector resolution of L and W results in a side force F, which causes the airplane to accelerate in the direction of F. This sidewise motion of the airplane is called a *slideslip*. Relative to the airplane, there appears a slideslip velocity V_S, shown in Fig. 7.40*b*.

Consider the effect of this slideslip velocity on the lift generated by the right and left wings. This is illustrated in Fig. 7.41. In Fig. 7.41*a*, the airplane is shown with the right and left wings in the same plane, perpendicular to the plane of symmetry of the fuselage. Let L_1 and L_2 be the lift generated by the right and left wings, respectively. The slideslip velocity V_S will affect the lift generated by each wing, but since the two wings are in the same plane, V_S makes the same angle θ with respect to both wings; therefore, $L_1 = L_2$, as shown in Fig. 7.41*a*. As a result, there is no restoring moment to return the airplane to its original equilibrium position, shown in Fig. 7.40*a*. However, consider the case where both wings are bent upward through angle Γ, as shown in Fig. 7.41*b*; that is, the wings are designed with a V shape. This is called *dihedral,* and Γ is the dihedral

DESIGN BOX

For a given airplane design, the amount of dihedral depends on the location of the wing relative to the fuselage, that is, low-wing, midwing, or high-wing location. The schematics in Figs. 7.40 and 7.41 show a low-wing design. More dihedral is needed for a low-wing position than for a midwing or high-wing position. Also, a swept-back wing requires less dihedral than a straight wing. Some degree of lateral stability is usually necessary in conventional airplanes but too much makes the airplane very sluggish to aileron control inputs. Indeed, the combination of mid- or high-wing location along with sweepback may have too much inherent lateral stability, and *anhedral* (negative dihedral) must be used to counteract some of this. Raymer (see Bibliography) gives the following typical values of dihedral (and anhedral) angle (in degrees) for various classes of airplanes:

	Wing Position		
	Low	**Middle**	**High**
Unswept (civil)	5 to 7	2 to 4	0 to 2
Subsonic swept wing	3 to 7	−2 to 2	−5 to −2
Supersonic swept wing	0 to 5	−5 to 0	−5 to 0

The amount of dihedral shown in Fig. 7.41*b* is greatly exaggerated for the purpose of illustration. The amount of dihedral (or anhedral) for some actual airplanes can be seen from the three views shown earlier in this book, that is, the F-86 (Fig. 2.15), the F4U Corsair (Fig. 2.16), the X-29 (Fig. 2.19), the F3F (Fig. 2.20), the F-104 (Fig. 4.45), the X-1 (Fig. 5.28), the U-2 (Fig. 5.49), the English Electric Lightning (Fig. 5.58), the Mirage C (Fig. 5.62), the Concorde (Fig. 5.63), and the P-38 (Fig. 7.42).

angle. Here, the slideslip velocity makes an angle θ_1 with respect to the right wing and a larger angle θ_2 with respect to the left wing. As a result, the lift on the left wing L_2 is smaller than the lift on the right wing, and this creates a restoring rolling moment that tends to return the airplane to its equilibrium position, as shown in Fig. 7.41*b*. Hence, *dihedral is the design feature of the airplane that provides lateral stability.*

There are more sophisticated explanations of the dihedral effect. Also, there is always a coupling between yawing and rolling motion, so that one does not occur without the other. It is beyond the scope of this book to go into these matters further. You will examine these effects when you embark on a more advanced study of stability and control. The function of this section and Sec. 7.17 has been only to introduce some of the most basic thoughts about directional and lateral stability.

7.19 A COMMENT

This brings to a close our technical discussion of stability and control. The preceding sections constitute an introduction to the subject; however, we have just scratched the surface. There are many other considerations: control forces, dynamic stability, etc. Such matters are the subject of more advanced studies of stability and control and are beyond the scope of this book. However, this subject is one of the fundamental pillars of aeronautical engineering, and the interested reader can find extensive presentations in books such as those of Perkins and Hage, and Etkin (see Bibliography at the end of this chapter).

7.20 HISTORICAL NOTE: THE WRIGHT BROTHERS VERSUS THE EUROPEAN PHILOSOPHY ON STABILITY AND CONTROL

The two contrasting scenes depicted in Sec. 7.1—the lumbering, belabored flight of Farman versus the relatively effortless maneuvering of Wilbur Wright—underscore two different schools of aeronautical thought during the first decade of powered flight. One school, consisting of virtually all early European and U.S. aeronautical engineers, espoused the concept of inherent stability (statically stable aircraft); the other, consisting solely of Wilbur and Orville Wright, practiced the design of statically unstable aircraft that had to be controlled every instant by the pilot. Both philosophies have their advantages and disadvantages, and because they have an impact on modern airplane design, we examine their background more closely.

The basic principles of airplane stability and control began to evolve at the time of George Cayley. His glider of 1804, sketched in Fig. 1.8, incorporated a vertical and horizontal tail that could be adjusted up and down. In this fashion, the complete tail unit acted as an elevator.

The next major advance in airplane stability was made by Alphonse Penaud, a brilliant French aeronautical engineer who committed suicide in 1880 at the age of 30. Penaud built small model airplanes powered by twisted rubber bands, a precursor of the flying balsa-and-tissue paper models of today. Penaud's design had a fixed wing and tail, like Cayley's, even though at the time Penaud was not aware of Cayley's work. Of particular note was Penaud's horizontal tail design, which was set at a negative 8° with respect to the wing chord line. Here we find the first true understanding of the role of the tail-setting angle i_t (see Secs. 7.5 and 7.7) on the static stability of an airplane. Penaud flew his model in the Tuileries Gardens in Paris on August 18, 1871, before members of the Société de Navigation Aérienne. The aircraft flew for 11 s, covering 131 ft. This event, along with Penaud's theory for stability, remained branded on future aeronautical designs right down to the present.

After Penaud's work, the attainment of "inherent" (static) stability became a dominant feature in aeronautical design. Lilienthal, Pilcher, Chanute, and Langley all strived for it. However, static stability has one disadvantage: The more stable the airplane, the harder it is to maneuver. An airplane that is highly stable is also sluggish in the air; its natural tendency to return to equilibrium somewhat defeats the purpose of the pilot to change its direction by means of control deflections. The Wright brothers recognized this problem in 1900. Since Wilbur and Orville were *airmen* in the strictest meaning of the word, they aspired for quick and easy maneuverability. Therefore, they discarded the idea of inherent stability that was entrenched by Cayley and Penaud. Wilbur wrote that "we . . . resolved to try a fundamentally different principle. We would arrange the machine so that it would not tend to right itself." The Wright brothers designed their aircraft to be statically unstable! This feature, along with their development of lateral control through wing warping, is primarily responsible for the fantastic

aerial performance of all their airplanes from 1903 to 1912 (when Wilbur died). Of course, this design feature heavily taxed the pilot, who had to keep the airplane under control at every instant, continuously operating the controls to compensate for the unstable characteristics of the airplane. Thus, the Wright airplanes were difficult to fly, and long periods were required to train pilots for these aircraft. In the same vein, such unstable aircraft were more dangerous.

These undesirable characteristics were soon to be compelling. After Wilbur's dramatic public demonstrations in France in 1908 (see Sec. 1.8), the European designers quickly adopted the Wrights' patented concept of combined lateral and directional control by coordinated wing warping (or by ailerons) and rudder deflection. But they rejected the Wrights' philosophy of static instability. By 1910, the Europeans were designing and flying aircraft that properly mated the Wrights' control ideas with the long-established static stability principles. However, the Wrights stubbornly clung to their basic unstable design. As a result, by 1910 the European designs began to surpass the Wrights' machines, and the lead in aeronautical engineering established in the United States in 1903 now swung to France, England, and Germany, where it remained for almost 20 years. In the process, static stability became an unquestioned design feature in all successful aircraft up to the 1970s.

It is interesting that very modern airplane design has returned full circle to the Wright brothers' original philosophy, at least in some cases. Recent lightweight military fighter designs, such as the F-16 and F-18, are statically unstable in order to obtain dramatic increases in maneuverability. At the same time, the airplane is instantaneously kept under control by computer-calculated and electrically adjusted positions of the control surfaces—the *fly-by-wire* concept. In this fashion, the maneuverability advantages of static instability can be realized without heavily taxing the pilot: The work is done by electronics! Even when maneuverability is not a prime feature, such as in civil transport airplanes, static instability has some advantages. For example, the tail surfaces for an unstable airplane can be smaller, with a subsequent savings in structural weight and reductions in aerodynamic drag. Hence, with the advent of the fly-by-wire system, the cardinal airplane design principle of static stability may be somewhat relaxed in the future. The Wright brothers may indeed ride again!

7.21 HISTORICAL NOTE: THE DEVELOPMENT OF FLIGHT CONTROLS

Figure 7.3 illustrates the basic aerodynamic control surfaces on an airplane—the ailerons, elevator, and rudder. They have been an integral part of airplane designs for most of the 20th century, and we take them almost for granted. But where are their origins? When did such controls first come into practical use? Who had the first inspirations for such controls?

In Sec. 7.20, we already mentioned that by 1809 George Cayley employed a movable tail in his designs, the first effort at some type of longitudinal control. Cayley's idea of moving the complete horizontal tail to obtain such control

persisted through the first decade of the 20th century. Henson, Stringfellow, Penaud, Lilienthal, and the Wright brothers all envisioned or utilized movement of the complete horizontal tail surface for longitudinal control. It was not until 1908 to 1909 that the first "modern" tail control configuration was put into practice. This was achieved by the French designer Levavasseur on his famous Antoinette airplanes, which had fixed vertical and horizontal tail surfaces with movable, flaplike rudder and elevator surfaces at the trailing edges. So the configuration for elevators and rudders shown in Fig. 7.3 dates back to 1908, five years after the dawn of powered flight.

The origin of ailerons (a French word for the extremity of a bird's wing) is steeped in more history and controversy. It is known that the Englishman M. P. W. Boulton patented a concept for lateral control by ailerons in 1868. Of course, at that time no practical aircraft existed, so the concept could not be demonstrated and verified, and Boulton's invention quickly retreated to the background and was forgotten. Ideas of warping the wings or inserting vertical surfaces (spoilers) at the wing tips cropped up several times in Europe during the late 19th century and into the first decade of the 20th century, but always in the context of a braking surface that would slow one wing down and pivot the airplane about a vertical axis. The true function of ailerons or wing warping, that for lateral control for banking and consequently turning an airplane, was not fully appreciated until Orville and Wilbur incorporated wing warping on their *Flyers* (see Chap. 1). The Wright brothers' claim that they were the first to invent wing warping may not be historically precise, but clearly they were the first to demonstrate its function and to obtain a legally enforced patent on its use (combined with simultaneous rudder action for total control in banking). The early European airplane designers did not appreciate the need for lateral control until Wilbur's dramatic public flights in France in 1908. This is in spite of the fact that Wilbur had fully described their wing warping concept in a paper at Chicago on September 1, 1901, and again on June 24, 1903; indeed, Octave Chanute clearly described the Wrights' concept in a lecture to the Aero Club de France in Paris in April 1903. Other aeronautical engineers at that time, if they listened, did not pay much heed. As a result, European aircraft before 1908, even though they were making some sustained flights, were awkward to control.

However, the picture changed after 1908, when in the face of the indisputable superiority of the Wrights' control system, virtually everybody turned to some type of lateral control. Wing warping was quickly copied and was employed on numerous different designs. Moreover, the idea was refined to include movable surfaces near the wing tips. These were first separate "winglets" mounted either above, below, or between the wings. But in 1909, Henri Farman (see Sec. 7.1) designed a biplane named the *Henri Farman III,* that included a flaplike aileron at the trailing edge of all four wing tips; this was the true ancestor of the conventional modern-day aileron, as sketched in Fig. 7.3. Farman's design was soon adopted by most designers, and wing warping quickly became passé. Only the Wright brothers clung to their old concept; a Wright airplane did not incorporate ailerons until 1915, six years after Farman's development.

7.22 HISTORICAL NOTE: THE "TUCK-UNDER" PROBLEM

A quick examination of Fig. 7.21, and the resulting stability equations such as Eqs. (7.26), (7.27), and (7.28), clearly underscores the importance of the downwash angle ε in determining longitudinal static stability. Downwash is a rather skittish aerodynamic phenomenon, very difficult to calculate accurately for real airplanes and therefore usually measured in wind tunnel tests or in free flight. A classic example of the stability problems that can be caused by downwash, and how wind tunnel testing can help, occurred during World War II, as described in the following.

In numerous flights during 1941 and 1942, the Lockheed P-38, a twin-engine, twin-boomed, high-performance fighter plane (see Fig. 7.42), went into sudden dives from which recovery was exceptionally difficult. Indeed, several pilots

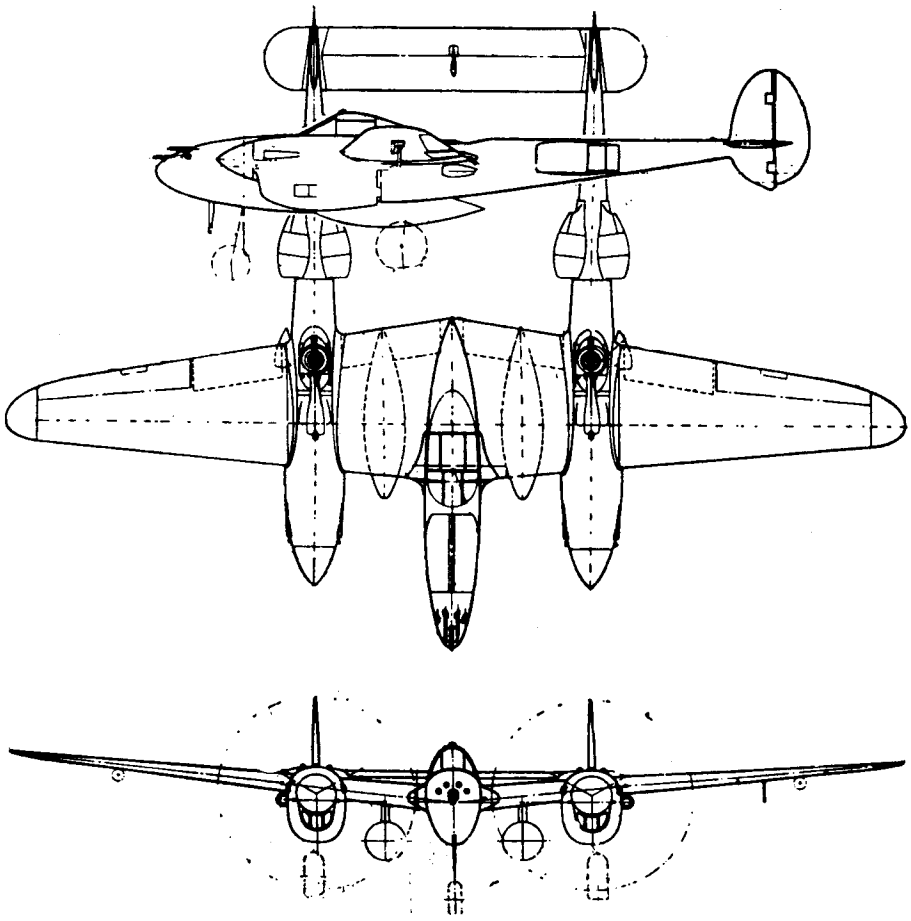

Figure 7.42 The Lockheed P-38 of World War II fame.

were killed in this fashion. The problem occurred at high subsonic speeds, usually in a dive, where the airplane had a tendency to nose over, putting the plane in yet a steeper dive. Occasionally, the airplane would become locked in this position, and even with maximum elevator deflection, a pullout could not be achieved. This "tuck-under" tendency could not be tolerated in a fighter aircraft that was earmarked for a major combat role.

Therefore, with great urgency, NACA was asked to investigate the problem. Since the effect occurred only at high speeds, usually above Mach 0.6, compressibility appeared to be the culprit. Tests in the Langley 30-ft by 60-ft low-speed tunnel and in the 8-ft high-speed tunnel (see Sec. 4.24) correlated the tuck-under tendency with the simultaneous formation of shock waves on the wing surface. Such compressibility effects were discussed in Secs. 5.9 and 5.10, where it was pointed out that beyond the critical Mach number for the wing, shock waves will form on the upper surface, encouraging flow separation far upstream of the trailing edge. The P-38 was apparently the first operational airplane to encounter this problem. The test engineers at Langley made several suggestions to rectify the situation, but all involved major modifications of the airplane. For a model already in production, a quicker fix was needed.

Next, the 16-ft high-speed wind tunnel at the NACA Ames Aeronautical Laboratory in California (see again Sec. 4.24) was pressed into service on the P-38 problem. Here, further tests indicated that the shock-induced separated flow over the wing was drastically reducing the lift. In turn, because the downwash is directly related to lift, as discussed in Secs. 5.13 and 5.14, the downwash angle ε was greatly reduced. Consequently (see Fig. 7.21), the tail angle of attack α_t was markedly increased. This caused a sharp increase in the positive lift on the tail, creating a strong pitching moment, nosing the airplane into a steeper dive. After the series of Ames tests in April 1943, Al Erickson of NACA suggested the addition of flaps on the lower surface of the wing at the $0.33c$ point in order to increase the lift, hence increase the downwash. This was the quick fix that Lockheed was looking for, and it worked.

7.23 Summary

Some of the important points of this chapter are given as follows.

1. If the forces and moments on a body caused by a disturbance tend *initially* to return the body *toward* its equilibrium position, the body is statically stable. In contrast, if these forces and moments tend *initially* to move the body *away from* its equilibrium position, the body is *statically unstable.*
2. The necessary criteria for longitudinal balance and static stability are (a) $C_{M,0}$ must be positive, (b) $\partial C_{M,\text{cg}}/\partial \alpha_a$ must be negative, and (c) the trim angle of attack α_e must fall within the flight range of angle of attack for the airplane. These criteria may be evaluated quantitatively for a given airplane from

$$C_{M,0} = C_{M,\text{ac}_{\text{wb}}} + V_H a_t (i_t + \varepsilon_0) \tag{7.27}$$

and

$$\frac{\partial C_{M,\text{cg}}}{\partial \alpha_a} = a\left[h - h_{\text{ac}_{\text{wb}}} - V_H \frac{a_t}{a}\left(1 - \frac{\partial \varepsilon}{\partial \alpha}\right)\right] \tag{7.28}$$

where the tail volume ratio is given by

$$V_H = \frac{l_t S_t}{cS}$$

3. The neutral point is that location of the center of gravity where $\partial C_{M,\text{cg}}/\partial \alpha_a = 0$. It can be calculated from

$$h_n = h_{\text{ac}_{\text{wb}}} + V_H \frac{a_t}{a}\left(1 - \frac{\partial \varepsilon}{\partial \alpha}\right) \tag{7.30}$$

4. The static margin is defined as $h_n - h$. For static stability, the location of the center of gravity must be ahead of the neutral point; that is, the static margin must be positive.
5. The effect of elevator deflection δ_e on the pitching moment about the center of gravity is given by

$$C_{M,\text{cg}} = C_{M,\text{ac}_{\text{wb}}} + C_{L,\text{wb}}(h - h_{\text{ac}}) - V_H\left(a_t \alpha_t + \frac{\partial C_{L,t}}{\partial \delta_e}\delta_e\right) \tag{7.37}$$

6. The elevator deflection necessary to trim an airplane at a given angle of attack α_n is

$$\delta_{\text{trim}} = \frac{C_{M,0} + (\partial C_{M,\text{cg}}/\partial \alpha_a)\alpha_n}{V_H(\partial C_{L,t}/\partial \delta_e)} \tag{7.43}$$

Bibliography

Etkin, B.: *Dynamics of Flight,* Wiley, New York, 1959.

Gibbs-Smith, C. H.: *Aviation: An Historical Survey from Its Origins to the End of World War II,* Her Majesty's Stationery Office, London, 1970.

Perkins, C. D., and R. E. Hage: *Airplane Performance, Stability, and Control,* Wiley, New York, 1949.

Raymer, D. P.: *Aircraft Design: A Conceptual Approach,* 3d ed., American Institute of Aeronautics and Astronautics, Reston, VA, 1999.

Problems

7.1 For a given wing-body combination, the aerodynamic center lies 0.03 chord length ahead of the center of gravity. The moment coefficient about the center of gravity is 0.0050, and the lift coefficient is 0.50. Calculate the moment coefficient about the aerodynamic center.

7.2 Consider a model of a wing-body shape mounted in a wind tunnel. The flow conditions in the test section are standard sea-level properties with a velocity of 100 m/s. The wing area and chord are 1.5 m^2 and 0.45 m, respectively. Using the wind tunnel force and moment-measuring balance, the moment about the center of gravity when the lift is zero is found to be -12.4 N · m. When the model is pitched to another angle of attack, the lift and moment about the center of gravity are measured to be 3675 N and 20.67 N · m, respectively. Calculate the value of the moment coefficient about the aerodynamic center and the location of the aerodynamic center.

7.3 Consider the model in Prob. 7.2. If a mass of lead is added to the rear of the model such that the center of gravity is shifted rearward by a length equal to 20 percent of the chord, calculate the moment about the center of gravity when the lift is 4000 N.

7.4 Consider the wing-body model in Prob. 7.2. Assume that a horizontal tail with no elevator is added to this model. The distance from the airplane's center of gravity to the tail's aerodynamic center is 1.0 m. The area of the tail is 0.4 m^2, and the tail-setting angle is 2.0°. The lift slope of the tail is 0.12 per degree. From experimental measurement, $\varepsilon_0 = 0$ and $\partial\varepsilon/\partial\alpha = 0.42$. If the absolute angle of attack of the model is 5° and the lift at this angle of attack is 4134 N, calculate the moment about the center of gravity.

7.5 Consider the wing-body-tail model of Prob. 7.4. Does this model have longitudinal static stability and balance?

7.6 For the configuration of Prob. 7.4, calculate the neutral point and static margin. $h = 0.26$.

7.7 Assume that an elevator is added to the horizontal tail of the configuration given in Prob. 7.4. The elevator control effectiveness is 0.04. Calculate the elevator deflection angle necessary to trim the configuration at an angle of attack of 8°.

7.8 Consider the configuration of Prob. 7.7. The elevator hinge moment derivatives are $\partial C_{h_e}/\partial\alpha_t = -0.007$ and $\partial C_{h_e}/\partial\delta_e = -0.012$. Assess the stick-free static stability of this configuration.

7.9 Consider the canard configuration as illustrated in Fig. 7.17*b*, and represented by the XB-70 shown in Fig. 7.18. You will sometimes encounter a statement, either written or verbal, that the canard configuration is inherently statically unstable. This is absolutely not true. Prove that the canard configuration can be made statically stable. What design condition must hold to insure its stability?